DESIGN AND OPTIMIZATION OF NONLINEAR VIBRATION ISOLATOR IN TWO DEGREES OF FREEDOM

by

Sarp Gönülkırmaz

Submitted to Graduate School of Natural and Applied Sciences
in Partial Fulfillment of the Requirements
for the Degree of Master of Science in
Mechanical Engineering

Yeditepe University

2022

DESIGN AND OPTIMIZATION OF NONLINEAR VIBRATION ISOLATOR IN TWO DEGREES OF FREEDOM

APPROVED BY:

Prof. Dr. Mehmet A. Akgün ……
(Thesis Supervisor)
(Yeditepe University)

Prof. Dr. Ata Muğan ……
(Istanbul Technical University)

Assist. Prof. Dr. Namık Cıblak ……
(Yeditepe University)

DATE OF APPROVAL: ..../..../20..

I hereby declare that this thesis is my own work and that all information in this thesis has been obtained and presented in accordance with academic rules and ethical conduct. I have fully cited and referenced all material and results as required by these rules and conduct, and this thesis study does not contain any plagiarism. If any material used in the thesis requires copyright, the necessary permissions have been obtained. No material from this thesis has been used for the award of another degree.

I accept all kinds of legal liability that may arise in case contrary to these situations.

Name, Last name Sarp Gönülkırmaz

Signature ……..……..

ACKNOWLEDGEMENTS

I hereby acknowledge all the profound support I've been given by Professor Mehmet A. Akgün, who took me under his guidance, starting from the second year of my Bachelor's. He guided me not only down the academic path but also down the path of life. Professor Mehmet A. Akgün has my immense gratitude, now and forever.

I would also like to express my gratitude to Professor Ali Bahadır Olcay, who has always been kind, understanding, and supportive of all his students, and Assist. Professor Namık Cıblak, who welcomes all kinds of intellectual discussions and takes great pleasure in enlightening his students.

I thank all the academic and administrative staff of Yeditepe University, Mechanical Engineering Department. I enjoyed my time as a teaching assistant profoundly and always felt like I belonged.

Lastly, I want to thank my close family, who always support my academic endeavors.

ABSTRACT

DESIGN AND OPTIMIZATION OF NONLINEAR VIBRATION ISOLATOR IN TWO DEGREES OF FREEDOM

Mechanical vibrations affect all manner of structures and systems. Vibration effects are usually not desired; they might cause fatigue, sudden failure, or affect sensitive sensors. Vibration isolators are essential components that suppress or eliminate vibration effects. Towards this goal, many types of active and passive vibration isolators exist. Passive isolators have two main categories, which are linear and nonlinear. The type which is being discussed throughout this thesis is of the passive nonlinear type. More specifically, it is a type of high-static-low-dynamic-stiffness, hardening, and nonlinear due to geometry vibration isolator in two degrees of freedom. Single degree of freedom quasi zero stiffness (SDOF QZS) isolators are also a part of this type. The optimization and performance of SDOF QZS isolators are well established. However, they are not suited to handle excitation on two axes. Therefore optimization and performance of a more general type in two degrees of freedom isolator is investigated. The isolator is considered with simple linear springs, but the geometry of the springs causes inherent nonlinearities. Optimization is carried out using genetic algorithms in conjunction with a Runge-Kutta numeric solver because of the nonlinear nature of the isolator. The algorithm of the optimization process is laid out and benchmarked against an equivalent QZS isolator.

ÖZET

İKİ ÖZGÜRLÜK DERECESİNE SAHİP LİNEER OLMAYAN BİR TİTREŞİM SÖNÜMLEYİCİSİNİN TASARIM VE OPTİMİZASYONU

Mekanik titreşimler pek çok yapıyı ve sistemi etkilemektedirler. Titreşim etkileri genellikle arzu edilmeyen etkilerdir; metal yorgunluğuna, ani kırılmalara sebep olup, hassas sensörlerin ölçümlerini etkileyebilirler. Titreşim sönümleyicileri titreşim etkilerini baskılayan veya ortadan kaldıran önemli komponentlerdir. Bu amaca hizmet eden, pek çok aktif veya pasif titreşim sönümleyicisi tipi bulunmaktadır. Pasif titreşim sönümleyicilerinin iki ana tipi bulunmaktadır. Bunlar lineer ve lineer olmayan tiplerdir. Bu tezde tartışılan tip, pasif lineer olmayan tiptir. Daha spesifik olmak gerekirse, yüksek-statik-düşük-dinamik sertliğe sahip, çekme ile sertleşen, ve geometri kaynaklı olarak lineer olmayan tiptir. Tek özgürlük dereceli, sıfırımsı sertlik (TÖD SS) sönümleyiciler de bu grubun altında yeralmaktadırlar. TÖD SS sönümleyicilerin optimizasyon ve performans ölçümlemeleri litaratüre iyi yerleşmiştir. Ancak iki eksenden gelen etkilere karşı uygun değillerdir. Bu sebep ile iki özgürlük derecesine sahip daha genel bir tipin araştırılması yapılmıştır. Sönümleyici basit lineer yaylar kullanılarak tasarlanmış, ancak geometrik ilişkiden kaynaklı olarak lineer olmayan hareket denklemleri ortaya çıkmıştır. Optimizasyon, genetik algoritmalar ve Runge-Kutta nümerik çözücüsü kullanılarak yapılmıştır. Optimizasyon algoritması açıklanmış ve denk bir TÖD SS sönümleyiciye karşı performans ölçümlemesi ortaya konmuştur.

TABLE OF CONTENTS

LIST OF FIGURES

LIST OF TABLES

LIST OF SYMBOLS/ABBREVIATIONS

m	Mass
k_o, k_v	Linear spring stiffness constants
c_o, c_v	Viscous damping coefficients
ω	Excitation frequency
$\vec{R}$	Position vector
a	Half width of the isolator
b	Half the height of the isolator
α	Stiffness ratio of the isolator
β	Geometric ratio of the isolator
L_o, L_v	Unstretch legth of springs
$\hat{K}_x$, $\hat{K}_y$	Normalized directional stiffnesses
$\hat{X}$, $\hat{Y}$	Normalized relative displacement
f_{mn}	Objective function
w_x, w_y	Directional optimization weights
μ_{mn}	Optimized set of parameters
$\boldsymbol{\lambda}_{mn}$	Objective function matrix

1. INTRODUCTION

Mechanical vibration is a phenomenon affecting almost all types of structures and machines caused by dynamic forces, either oscillatory or random. Dynamic forces may result from rotating machinery, such as engines, turbines, and motors; from the air in motion, such as wind in a central air conditioning system; from a vehicle or an aircraft moving on a rough surface; and from other various sources. Fluid dynamics effects, like cavities inside a pump, can also cause such dynamic excitations. Alternatively, as in the example of earthquakes, the cause may be tectonic movements. Although there are applications where vibration is utilized beneficially, it is usually an undesirable phenomenon. It can cause sudden failure of structures and mechanical parts, mainly when it induces resonance. Even when it does not induce resonance, it can still cause faster propagation of fatigue cracks, uncertainty in sensitive measurement equipment, or discomfort in the mildest cases. Therefore, it is imperative that this phenomenon must be well understood and accounted for.

In cases where vibration is undesired, it must be isolated to prevent detrimental effects. This process is called vibration isolation. Many different kinds of vibration isolators exist. For example, car suspensions isolate occupants from road surface imperfections, pylon attachment points in an aircraft isolate wings from engine vibration, special mounting points in some bridges isolate the structure from earthquakes, and rubber mountings of an electric motor minimize vibration transmitted to the base on which the motor is mounted. Demands from a vibration isolator vary depending on the structure's mass, the equipment's functionality, and the excitation force's frequency and amplitude. In general, performance demands are higher than ever before, with lower tolerances in manufacturing and the expectation of higher efficiency in all applications.

1.1. PASSIVE VIBRATION ISOLATION

Vibration isolators fall into two categories, namely, active and passive. Active systems monitor excitation signals and manage isolator parameters actively. Therefore, active systems have some control feedback built into them and usually perform better in isolation metrics. However, they are delicate, expensive, require frequent maintenance, and are impractical for large systems and structures. Passive isolators, on the other hand, have fixed

design parameters. Therefore, simple passive isolators can only be effective under a narrower set of excitation conditions. But they are robust, almost maintenance-free, and inexpensive. Passive vibration isolators are the focus of this thesis.

Passive vibration isolators are usually designed under linearity assumptions. This assumption allows for straightforward analysis and enables analytical solutions to be put forward mathematically. However, as discussed in this chapter, there are limitations to linearity. Linearity limitation can manifest itself as either the divergence between the real-world testing and mathematical solutions or the inability to provide a set of design parameters that satisfy the performance threshold. Nonlinear analysis, however, has its own set of difficulties. The main drawback is that it is not possible to put forward an analytical solution. Hence, the optimization of design parameters provides a challenge. This challenge is overcome with other assumptions, like modeling the system as a Duffing Oscillator [1], or relying on numerical solutions, as is the case with this thesis.

A vibration isolator has two main performance measurement criteria. The first one is displacement transmissibility, which reflects how much of the base movement is transmitted to the system. The second one is the frequency at which isolation begins, meaning the frequency at which the system's movement is less than the base movement. Parallel to displacement transmissibility, there is also force transmissibility. These two are directly related to one another for a linear isolator. However, this direct relation is broken in the case of nonlinear isolators. Either or both of these metrics may be used to assess the performance of linear and nonlinear isolators. Large displacements are undesirable; however, large accelerations due to high frequencies are also of serious concern, even though displacement amplitudes may be small.

A simple single degree of freedom (SDOF) representation is how, at least initially, problems are often represented in the vibration isolation domain. Some simplifying assumptions, such as lumped mass, small displacements/angles, linear dampers, and springs, are made in most cases. Such a model is often the preliminary step for isolator design.

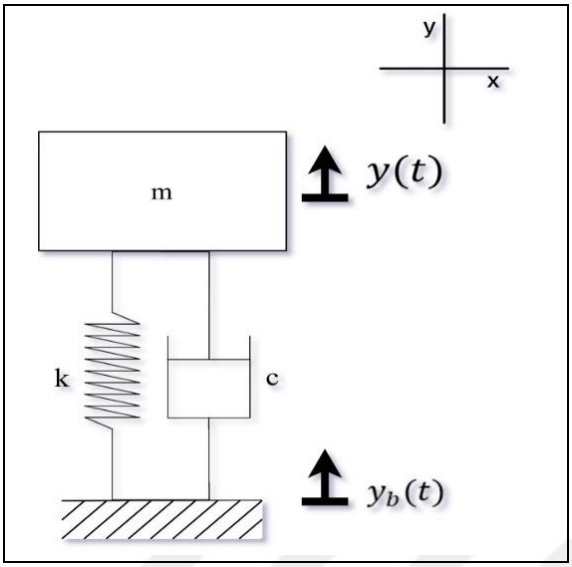

Figure 1.1: SDOF base excitation

An SDOF base excitation problem is given in Fig. 1. Excitation caused by the vibration source is represented with $y_b(t)$ and the response of the mass is represented by $y(t)$. The source and the mass are connected by a linear spring and damper. Both the excitation and the response are on a single axis. The governing differential equation for the response is given as

$$m\ddot{y} + c(\dot{y} - \dot{y}_b) + k(y - y_b) = 0 \tag{1.1}$$

Letting $y_b(t) = A\sin(\omega t)$, and considering $\dot{y}_b(t) = \omega A\cos(\omega t)$, the following is obtained:

$$m\ddot{y} + c\dot{y} + ky = c\omega A\cos(\omega t) + kA\sin(\omega t) \tag{1.2}$$

The left-hand side of Eq. (1.2) is a well-known second-order differential equation. On the right-hand side, there are two excitation functions. The term with k represents the force exerted by the spring, and the term with c represents the force exerted by the damper. Because the equation is linear, the response caused by each excitation term can be solved using the method of undetermined coefficients, and the two solutions can be superposed.

The steady-state solution reveals itself as

$$y(t) = \omega_n A\left(\frac{\omega_n^2 + (2\zeta\omega)^2}{(\omega_n^2 - \omega^2)^2 + (2\zeta\omega_n\omega)^2}\right)^{1/2} \cos(\omega t - \theta_1 - \theta_2) \tag{1.3}$$

Detailed work is present in [2], where natural frequency and damping ratio are defined as

$$\omega_n = \sqrt{\frac{k}{m}} \quad \text{and} \quad \zeta = \frac{c}{c_{cr}} \tag{1.4}$$

For vibration isolation purposes, it's useful to divide the steady-state amplitude by the base motion amplitude,

$$\left|\frac{B}{A}\right| = \left(\frac{1 + (2\zeta r)^2}{(1 - r^2)^2 + (2\zeta r)^2}\right)^{1/2} \tag{1.5}$$

where B stands for the amplitude of the response in Eq. (1.3) and

$$r = \frac{\omega}{\omega_n} \tag{1.6}$$

Equation (1.5) is called displacement transmissibility. A figure representing displacement transmissibility vs. frequency ratio can be found in [2]. From this figure, it can be seen that $B/A > 1$ for $r \leq \sqrt{2}$ and isolation starts at $r = \sqrt{2}$. This means the system is better at low frequencies without the isolator (i.e., without the combination of spring and the damper) than with it, which would not be a practical situation anyway. Resonance is the condition where r becomes unity for an undamped system, and for a damped system, resonance is around unity. In the case of an undamped system, the amplitude of the system response, therefore, the displacement ratio, goes to infinity in this state. Damping is added to the system to reduce the response amplitude around $r = 1$. However, this has the negative effect of increasing B/A at higher frequencies, where the damper becomes the main pathway of force transmission.

To conclude, a vibration isolator needs damping to prevent sudden failure around resonance but not so much that it affects high-frequency performance. At the same time, r needs to be as high as possible for the lowest amount of transmissibility. Looking at eq. (1.4) and eq. (1.6), smaller stiffness values result in lower transmissibility levels. However, it should be noted that isolators are also support structures for a system. Soft springs have high levels of static deflection, and it is impractical to use them. This is where the weakness of linear SDOF vibration isolator is. As an answer to this problem, high static low dynamic stiffness (HSLDS) isolators are proposed. They are a category of nonlinear vibration isolators with positive and negative stiffness members. Negative stiffness members are designed to become inert at equilibrium, allowing for high static stiffness. But, their effect becomes pronounced

with the dynamic response, causing softening in the resultant stiffness of the isolator. An HSLDS isolator is also the topic of this thesis.

1.2. AIM AND OBJECTIVES

This thesis aims to reduce vibration transmissibility by designing, modeling, and optimizing a nonlinear vibration isolator in two axes of motion. The cause for the nonlinearity is geometric relations and large deflections. To reach this aim, the following steps were undertaken.

- A two-degree-of-freedom (2DOF) system with excitation forces in both axes, wherein geometric nonlinearities were modeled.
- Analysis and optimization of the said model were conducted.
- The optimized proposed system was benchmarked against a comparable isolator.

1.3. OUTLINES

Following this section, a literature review of vibration isolation is presented in Chapter 2. In Chapter 3, a mathematical model for the system is developed, followed by Chapter 4, in which optimization of the system is conducted utilizing the genetic algorithm. The optimized isolator is benchmarked against a comparable system in Chapter 5. And finally, discussions and conclusions of the thesis are presented in Chapter 6.

2. LITERATURE REVIEW

Many different types of passive nonlinear vibration isolators exist, a comprehensive summary of which is presented in the work of Ibrahim [3]. Of all types, HSLDS isolators capture most of the interest in the passive nonlinear vibration isolation domain. HSLDS isolators are mainly made of two parts. The first one is usually a regular linear spring, placed vertically and provides support to the structure, and the second one is a negative stiffness structure consisting of two springs, which causes the nonlinearity.

The nonlinear components can be made out of linear springs, compressed initially, and placed horizontally, perpendicular to the main axis of motion, canceling each other out at equilibrium. The idea behind this configuration can be seen in references [1,4–6]. Nonlinearity in such isolators comes from the geometry. However, there are other methods as well, such as two repelling magnets being placed horizontally as “anti-springs”[4,7]. When the equilibrium condition is disturbed, the magnetic force starts acting on the vertical axis against the vertical spring, causing a softening effect. Euler buckled beams as negative stiffness members are another variation of this type [8,9]. Nonlinearity can be the result of a mechanism as well. Reference [10] considers scissor-like elements with linear springs in the middle. Alabuzhev [11] also lays out variations on such mechanisms. However, despite the variations, general concepts are the same for passive nonlinear isolators. This thesis focuses on the classical version containing compressed springs placed horizontally.

Parameters of an HSLDS isolator can be tuned in such a way that, at equilibrium, stiffness becomes “quasi” zero. These uniquely conditioned isolators are called Quasi-Zero Stifness isolators. Static and dynamic characteristics of QZS isolators for single degree of freedom systems were studied thoroughly in [4,5,12]. HSLDS isolators can be tuned to have a softening or hardening characteristic[4]. When a softening characteristic is present, the incremental recovering force gets smaller as displacement increases. A snap-through from the hardening region to the softening region in vibration around a static equilibrium position may occur, which is not desirable for stability reasons.

HSLDS isolators are usually modeled as Duffing Oscillators with cubic stiffness [1,4,5,13]. Solutions to the cubic stiffness problem are determined with Harmonic Balance Method, as laid out by Worden [14].

Single degree of freedom HSLDS isolators with hardening characteristics are studied thoroughly in the literature. However, these analytical solutions hold for SDOF only and disturbances rarely act on a single axis in real-life applications. Therefore, how an HSLDS system responds to excitation in two-DOF is a topic to be explored.

3. MATHEMATICAL MODEL

This thesis focuses on a nonlinear isolator with linear springs and dampers. Damping is modeled with viscous dampers. The nonlinearity of the isolator is an effect of geometric relations between the linear sub-components.

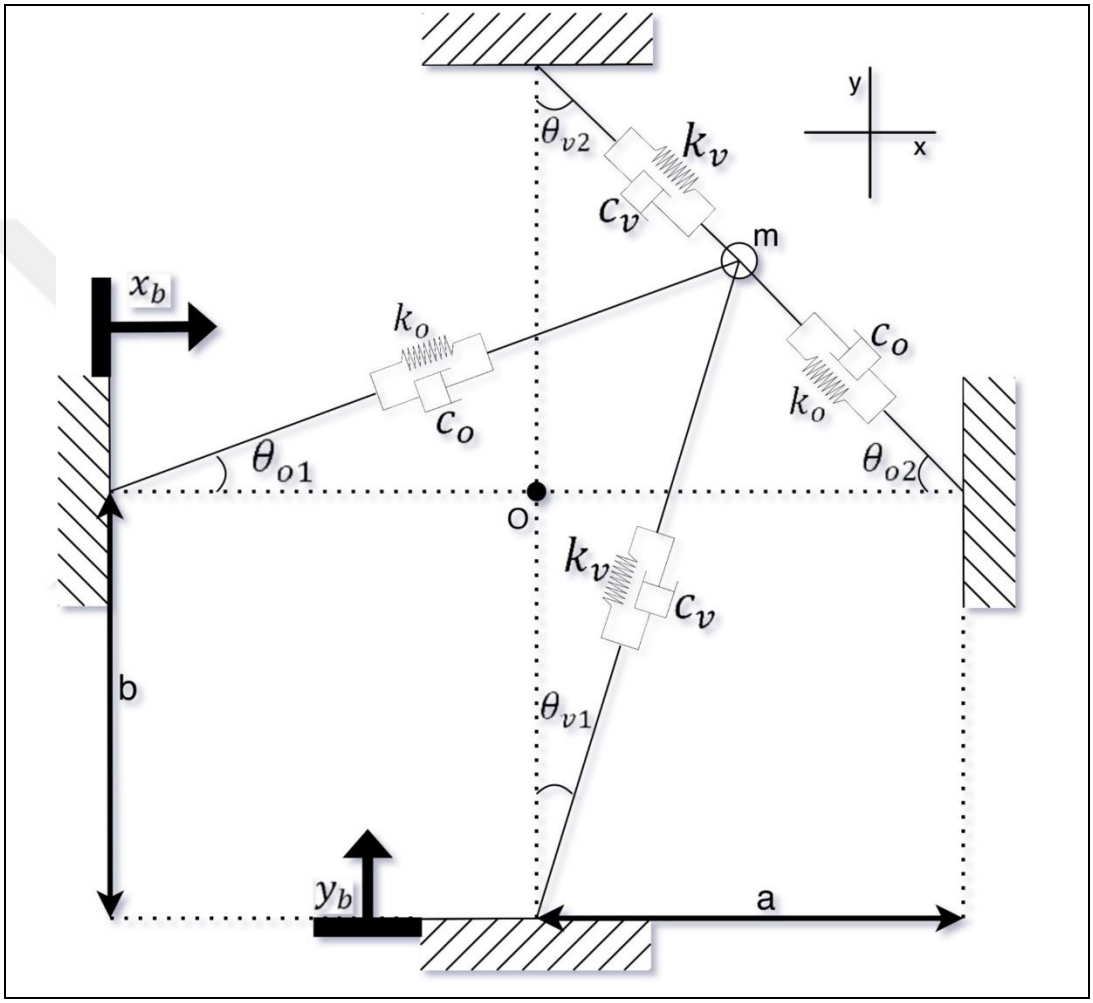

Figure 3.1. Two-degree-of-freedom isolator with dampers on all four sides. Mass m is at center O, the origin of the coordinate system, in static equilibrium.

Consider the system described in Figure 3.1., in which a mass is connected to four springs and four dampers. When in static equilibrium, the springs and dampers along the x-axis are described as oblique, and the ones along the y-axis as vertical. Numbering runs clockwise. Mass is modeled as a point mass. θ_{ij} represents one of the four angles at any given time, resulting from the motion of the point mass. Where i equals v or o for vertical and oblique,

and j equals 1 or 2 for the position, respectively. a is the distance from the origin to either of the vertical walls, while b is the distance from the origin to the top and bottom supports. The system is symmetric, and motion is always assumed to be $|x(t)| < a$ and $|y(t)| < b$, where $x(t)$ and $y(t)$ denote an arbitrary position of the mass measured with respect to point O, the fixed origin of the coordinate system (Fig. 3.1). Springs and dampers have the same stiffness and damping coefficient with respect to their orientations (i.e., $k_{v1} = k_{v2} = k_v$). Springs might initially be in tension, compression, or without any static loading.

A force may be applied to the mass, and the force transmission to the supports can be calculated. However, vibration is inflicted via base motion in this study. Bases on all four sides are connected to each other, and their motion is in phase. In other words, the bases may be thought of as the walls of a rigid box enclosing the system. Therefore, the motion of the box can be described with a single vector with no rotation, such as

$$\vec{R}_{base} = x_b(t)i + y_b(t)j \tag{3.1}$$

In Figure 3.2, a vector representation of the position of the point mass at an arbitrary instant due to base motion is given.

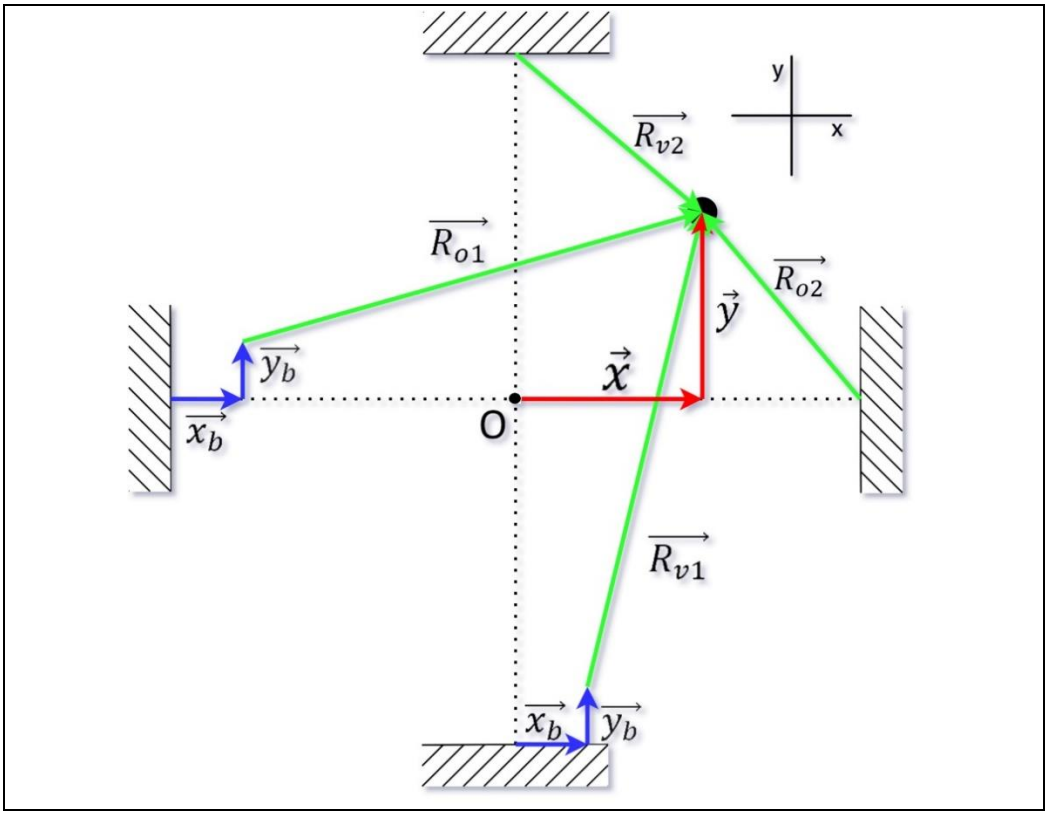

Figure 3.2. Vector representation of the position of the mass

Combining terms in the following manner will facilitate analysis.

$$X(t) = x(t) - x_b(t),\ Y(t) = y(t) - y_b(t),\ \dot{X}(t) = \dot{x}(t) - \dot{x}_b(t)$$
$$\text{and } \dot{Y}(t) = \dot{y}(t) - \dot{y}_b(t) \tag{3.2}$$

3.1. VECTOR REPRESENTATION OF SPRING ORIENTATIONS

The summation of vectors in a closed polygon should equal zero. Hence, this summation allows the derivation of $\vec{R}_{ij}$ which represent the orientation and length of the four springs at an arbitrary instant of time during vibration.

It follows for $\vec{R}_{o1}$, which is the vector for the first (i.e., the left) oblique spring (Fig 3.1), that

$$-ai + x_b(t)i + y_b(t)j + \vec{R}_{o1}(t) - y(t)j - x(t)i = 0 \tag{3.3}$$

where all arguments t are dropped. Rearranging,

$$\vec{R}_{o1} = (x - x_b + a)i + (y - y_b)j \tag{3.4}$$

The first derivative of vectors $\vec{R}_{ij}$ will become useful later when calculating damping forces. Hence,

$$\dot{\vec{R}}_{o1} = (\dot{x} - \dot{x}_b)i + (\dot{y} - \dot{y}_b)j \tag{3.5}$$

The unit vector along the direction of the first oblique spring is given by

$$\vec{r}_{o1} = \frac{\vec{R}_{o1}}{|\vec{R}_{o1}|} = \frac{X + a}{|\vec{R}_{o1}|}i + \frac{Y}{|\vec{R}_{o1}|}j \tag{3.6}$$

The length of the first oblique spring at an arbitrary instant of time is, therefore,

$$|\vec{R}_{o1}| = \sqrt{(x - x_b + a)^2 + (y - y_b)^2} \tag{3.7}$$

Similarly for $\vec{R}_{o2}$

$$+ai + x_bi + y_bj + \vec{R}_{o2} - yj - xi = 0 \tag{3.9}$$

With steps similar to those for the first oblique spring, a series of expressions are obtained as follows:

$$\vec{R}_{o2} = (x - x_b - a)i + (y - y_b)j \tag{3.10}$$

Differentiating vector $\vec{R}_{o2}$,

$$\dot{\vec{R}}_{o2} = (\dot{x} - \dot{x}_b)i + (\dot{y} - \dot{y}_b)j \tag{3.11}$$

Unit vector of $\vec{R}_{o2}$ is represented as

$$\vec{r}_{o2} = \frac{\vec{R}_{o2}}{|\vec{R}_{o2}|} = \frac{X - a}{|\vec{R}_{o2}|}i + \frac{Y}{|\vec{R}_{o2}|}j \tag{3.12}$$

The amplitude of the vector $\vec{R}_{o2}$ is,

$$|\vec{R}_{o2}| = \sqrt{(x - x_b - a)^2 + (y - y_b)^2} \tag{3.13}$$

Similarly for $\vec{R}_{v1}$, which is the vector for the first (i.e., the lower) vertical spring (Fig 3.1),

$$-bj + x_b i + y_b + \vec{R}_{v1} - yj - xi = 0 \tag{3.14}$$

$$\vec{R}_{v1} = (x - x_b)i + (y - y_b + b)j \tag{3.15}$$

Differentiating vector $\vec{R}_{v1}$,

$$\dot{\vec{R}}_{v1} = (\dot{x} - \dot{x}_b)i + (\dot{y} - \dot{y}_b)j \tag{3.16}$$

Unit vector of $\vec{R}_{v1}$ is represented as

$$\vec{r}_{v1} = \frac{\vec{R}_{v1}}{|\vec{R}_{v1}|} = \frac{X}{|\vec{R}_{v1}|}i + \frac{Y + b}{|\vec{R}_{v1}|}j \tag{3.17}$$

The amplitude of the vector $\vec{R}_{v1}$ is,

$$|\vec{R}_{v1}| = \sqrt{(x - x_b)^2 + (y - y_b + b)^2} \tag{3.18}$$

Similarly for $\vec{R}_{v2}$

$$+bj + x_b i + y_b + \vec{R}_{v2} - yj - xi = 0 \tag{3.19}$$

The following series of expressions follow steps similar to those above.

$$\vec{R}_{v2} = (x - x_b)i + (y - y_b - b)j \tag{3.20}$$

Differentiating vector $\vec{R}_{v2}$,

$$\dot{\vec{R}}_{v2} = (\dot{x} - \dot{x}_b)i + (\dot{y} - \dot{y}_b)j \tag{3.21}$$

Unit vector of $\vec{R}_{v2}$ is represented as

$$\vec{r}_{v2} = \frac{\vec{R}_{v2}}{|\vec{R}_{v2}|} = \frac{X}{|\vec{R}_{v2}|}i + \frac{Y - b}{|\vec{R}_{v2}|}j \tag{3.22}$$

The amplitude of the vector $\vec{R}_{v2}$ is,

$$|\vec{R}_{v2}| = \sqrt{(x - x_b)^2 + (y - y_b - b)^2} \tag{3.23}$$

3.2. EQUATIONS OF MOTION

With the previous definitions of vectors $\vec{R}_{ij}$, the equations of motion are derived in this section. It follows from Newton's second law that

$$-\vec{F}_{springs} - \vec{F}_{dampers} = m\vec{a} \tag{3.24}$$

The resultant force exerted by the four springs is given by

$$\vec{F}_{springs} = k_o\vec{\Delta}_{o1} + k_o\vec{\Delta}_{o2} + k_v\vec{\Delta}_{v1} + k_v\vec{\Delta}_{v2} \tag{3.25}$$

where, $\vec{\Delta}_{ij}$ is the change in length of spring ij at time t, represented as a vector in the direction of $\vec{R}_{ij}$. $\vec{\Delta}_{ij}$ can be written as

$$\vec{\Delta}_{o1} = \left(|\vec{R}_{o1}| - L_{o1}\right) \cdot \vec{r}_{o1} = \left(\sqrt{(X + a)^2 + (Y)^2} - L_{o1}\right) \cdot \vec{r}_{o1} \tag{3.26}$$

$$\vec{\Delta}_{o2} = \left(\left|\vec{R}_{o2}\right| - L_{o2}\right) \cdot \vec{r}_{o2} = \left(\sqrt{(X-a)^2 + (Y)^2} - L_{o2}\right) \cdot \vec{r}_{o2} \tag{3.27}$$

$$\vec{\Delta}_{v1} = \left(\left|\vec{R}_{v1}\right| - L_{v1}\right) \cdot \vec{r}_{v1} = \left(\sqrt{(X)^2 + (Y+b)^2} - L_{v1}\right) \cdot \vec{r}_{v1} \tag{3.28}$$

$$\vec{\Delta}_{v2} = \left(\left|\vec{R}_{v2}\right| - L_{v2}\right) \cdot \vec{r}_{v2} = \left(\sqrt{(X)^2 + (Y-b)^2} - L_{v2}\right) \cdot \vec{r}_{v2} \tag{3.29}$$

where L_{ij} is the undeformed length of spring ij. The resultant spring force $\vec{F}_{springs}$ then follows as

$$\begin{aligned}\vec{F}_{springs} = {} & k_o\left(\sqrt{(X+a)^2 + (Y)^2} - L_{o1}\right) \cdot \left(\frac{X+a}{\left|\vec{R}_{o1}\right|} i + \frac{Y}{\left|\vec{R}_{o1}\right|} j\right) \\ & + k_o\left(\sqrt{(X-a)^2 + (Y)^2} - L_{o2}\right) \cdot \left(\frac{X-a}{\left|\vec{R}_{o2}\right|} i + \frac{Y}{\left|\vec{R}_{o2}\right|} j\right) \\ & + k_v\left(\sqrt{(X)^2 + (Y+b)^2} - L_{v1}\right) \cdot \left(\frac{X}{\left|\vec{R}_{v1}\right|} i + \frac{Y+b}{\left|\vec{R}_{v1}\right|} j\right) \\ & + k_v\left(\sqrt{(X)^2 + (Y-b)^2} - L_{v2}\right) \cdot \left(\frac{X}{\left|\vec{R}_{v2}\right|} i + \frac{Y-b}{\left|\vec{R}_{v2}\right|} j\right)\end{aligned} \tag{3.30}$$

Carrying out the multiplications in equations (3.30) and separating the x and y components,

$$F_{springs_x} = \left[k_o\left(2X - L_{o1}\frac{X+a}{\left|\vec{R}_{o1}\right|} - L_{o2}\frac{X-a}{\left|\vec{R}_{o2}\right|}\right) + k_v\left(2X - L_{v1}\frac{X}{\left|\vec{R}_{v1}\right|} - L_{v2}\frac{X}{\left|\vec{R}_{v2}\right|}\right)\right] \tag{3.31}$$

$$F_{springs_y} = \left[k_o\left(2Y - L_{o1}\frac{Y}{\left|\vec{R}_{o1}\right|} - L_{o2}\frac{Y}{\left|\vec{R}_{o2}\right|}\right) + k_v\left(2Y - L_{v1}\frac{Y+b}{\left|\vec{R}_{v1}\right|} - L_{v2}\frac{Y-b}{\left|\vec{R}_{v2}\right|}\right)\right] \tag{3.32}$$

The resultant force exerted by dampers is given by

$$\begin{aligned}\vec{F}_{dampers} = {} & C_{o1}\left(\dot{\vec{R}}_{o1} \cdot \vec{r}_{o1}\right)\vec{r}_{o1} + C_{o2}\left(\dot{\vec{R}}_{o2} \cdot \vec{r}_{o2}\right)\vec{r}_{o2} + C_{v1}\left(\dot{\vec{R}}_{v1} \cdot \vec{r}_{v1}\right)\vec{r}_{v1} \\ & + C_{v2}\left(\dot{\vec{R}}_{v2} \cdot \vec{r}_{v2}\right)\vec{r}_{v2}\end{aligned} \tag{3.33}$$

Where a dot between two terms indicates a dot product.

Elaborating on the first oblique damper force $\vec{F}_{d_{o1}}$

$$\vec{F}_{d_{o1}} = C_{o1}\left(\dot{\vec{R}}_{o1} \cdot \vec{r}_{o1}\right)\vec{r}_{o1} \tag{3.34}$$

Substituting the relevant quantities,

$$\vec{F}_{d_{o1}} = C_{o1}\left(\left(\dot{X}i + \dot{Y}j\right) \cdot \left(\frac{X+a}{\left|\vec{R}_{o1}\right|}i + \frac{Y}{\left|\vec{R}_{o1}\right|}j\right)\right)\left(\frac{X+a}{\left|\vec{R}_{o1}\right|}i + \frac{Y}{\left|\vec{R}_{o1}\right|}j\right) \tag{3.35}$$

and performing the dot products,

$$\vec{F}_{d_{o1}} = C_{o1}\left(\frac{\dot{X}(X+a) + \dot{Y}Y}{\left|\vec{R}_{o1}\right|}\right)\left(\frac{X+a}{\left|\vec{R}_{o1}\right|}i + \frac{Y}{\left|\vec{R}_{o1}\right|}j\right) \tag{3.36}$$

That results in

$$\vec{F}_{d_{o1}} = C_{o1}\left(\frac{\dot{X}(X+a)^2 + \dot{Y}Y(X+a)}{\left|\vec{R}_{o1}\right|^2}\right)i + C_{o1}\left(\frac{\dot{X}Y(X+a) + \dot{Y}Y^2}{\left|\vec{R}_{o1}\right|^2}\right)j \tag{3.37}$$

Similar steps for $\vec{F}_{d_{o2}}$ lead to

$$\vec{F}_{d_{o2}} = C_{o2}\left(\dot{\vec{R}}_{o2} \cdot \vec{r}_{o2}\right)\vec{r}_{o2} \tag{3.38}$$

$$\vec{F}_{d_{o2}} = C_{o2}\left(\left(\dot{X}i + \dot{Y}j\right) \cdot \left(\frac{X-a}{\left|\vec{R}_{o2}\right|}i + \frac{Y}{\left|\vec{R}_{o2}\right|}j\right)\right)\left(\frac{X-a}{\left|\vec{R}_{o2}\right|}i + \frac{Y}{\left|\vec{R}_{o2}\right|}j\right) \tag{3.39}$$

$$\vec{F}_{d_{o2}} = C_{o2}\left(\frac{\dot{X}(X-a) + \dot{Y}Y}{\left|\vec{R}_{o2}\right|}\right)\left(\frac{X-a}{\left|\vec{R}_{o2}\right|}i + \frac{Y}{\left|\vec{R}_{o2}\right|}j\right) \tag{3.40}$$

$$\vec{F}_{d_{o2}} = C_{o2}\left(\frac{\dot{X}(X-a)^2 + \dot{Y}Y(X-a)}{\left|\vec{R}_{o2}\right|^2}\right)i + C_{o2}\left(\frac{\dot{X}Y(X-a) + \dot{Y}Y^2}{\left|\vec{R}_{o2}\right|^2}\right)j \tag{3.41}$$

Similarly for $\vec{F}_{d_{v1}}$

$$\vec{F}_{d_{v1}} = C_{v1}\left(\dot{\vec{R}}_{v1} \cdot \vec{r}_{v1}\right)\vec{r}_{v1} \tag{3.42}$$

$$\vec{F}_{d_{v1}} = C_{v1}\left(\left(\dot{X}i + \dot{Y}j\right)\cdot\left(\frac{X}{\left|\vec{R}_{v1}\right|}i + \frac{Y+b}{\left|\vec{R}_{v1}\right|}j\right)\right)\left(\frac{X}{\left|\vec{R}_{v1}\right|}i + \frac{Y+b}{\left|\vec{R}_{v1}\right|}j\right) \tag{3.43}$$

$$\vec{F}_{d_{v1}} = C_{v1}\left(\frac{\dot{X}X + \dot{Y}(Y+b)}{\left|\vec{R}_{v1}\right|}\right)\left(\frac{X}{\left|\vec{R}_{v1}\right|}i + \frac{Y+b}{\left|\vec{R}_{v1}\right|}j\right) \tag{3.44}$$

$$\vec{F}_{d_{v1}} = C_{v1}\left(\frac{\dot{X}X^2 + \dot{Y}X(Y+b)}{\left|\vec{R}_{v1}\right|^2}\right)i + C_{v1}\left(\frac{\dot{X}X(Y+b) + \dot{Y}(Y+b)^2}{\left|\vec{R}_{v1}\right|^2}\right)j \tag{3.45}$$

Finally for $\vec{F}_{d_{v2}}$

$$\vec{F}_{d_{v2}} = C_{v2}\left(\dot{\vec{R}}_{v2}\cdot\vec{r}_{v2}\right)\vec{r}_{v2} \tag{3.46}$$

$$\vec{F}_{d_{v2}} = C_{v2}\left(\left(\dot{X}i + \dot{Y}j\right)\cdot\left(\frac{X}{\left|\vec{R}_{v2}\right|}i + \frac{Y-b}{\left|\vec{R}_{v2}\right|}j\right)\right)\left(\frac{X}{\left|\vec{R}_{v2}\right|}i + \frac{Y-b}{\left|\vec{R}_{v2}\right|}j\right) \tag{3.47}$$

$$\vec{F}_{d_{v2}} = C_{v2}\left(\frac{\dot{X}X + \dot{Y}(Y-b)}{\left|\vec{R}_{v2}\right|}\right)\left(\frac{X}{\left|\vec{R}_{v2}\right|}i + \frac{Y-b}{\left|\vec{R}_{v2}\right|}j\right) \tag{3.48}$$

$$\vec{F}_{d_{v2}} = C_{v2}\left(\frac{\dot{X}X^2 + \dot{Y}X(Y-b)}{\left|\vec{R}_{v2}\right|^2}\right)i + C_{v2}\left(\frac{\dot{X}X(Y-b) + \dot{Y}(Y-b)^2}{\left|\vec{R}_{v2}\right|^2}\right)j \tag{3.49}$$

Although discussed to some extent, damping is not the main focus of this thesis. Therefore to simplify the upcoming analysis, only oblique 1 and vertical 1 dampers are considered. Hence, $C_{o1} = C_o$ and $C_{v1} = C_v$. The summation of all damping forces along the x and y axes is

$$F_{d_x} = \left(C_o\frac{\dot{X}(X+a)^2 + \dot{Y}Y(X+a)}{\left|\vec{R}_{o1}\right|^2} + C_v\frac{\dot{X}X^2 + \dot{Y}X(Y+b)}{\left|\vec{R}_{v1}\right|^2}\right) \tag{3.50}$$

$$F_{d_y} = \left(C_o \frac{\dot{X}Y(X+a) + \dot{Y}Y^2}{\left|\vec{R}_{o1}\right|^2} + C_v \frac{\dot{X}X(Y+b) + \dot{Y}(Y+b)^2}{\left|\vec{R}_{v1}\right|^2} \right) \tag{3.51}$$

Finally, equations (3.31), (3.32), (3.50), and (3.51) are plugged into equation (3.24) to obtain the equations of motion along the two axes.

$$\begin{aligned} m\ddot{x} + k_o \left(2X - L_{o1} \frac{X+a}{\left|\vec{R}_{o1}\right|} - L_{o2} \frac{X-a}{\left|\vec{R}_{o2}\right|} \right) + k_v \left(2X - L_{v1} \frac{X}{\left|\vec{R}_{v1}\right|} - L_{v2} \frac{X}{\left|\vec{R}_{v2}\right|} \right) \\ + C_o \frac{\dot{X}(X+a)^2 + \dot{Y}Y(X+a)}{\left|\vec{R}_{o1}\right|^2} + C_v \frac{\dot{X}X^2 + \dot{Y}X(Y+b)}{\left|\vec{R}_{v1}\right|^2} = 0 \end{aligned} \tag{3.52}$$

$$\begin{aligned} m\ddot{y} + k_o \left(2Y - L_{o1} \frac{Y}{\left|\vec{R}_{o1}\right|} - L_{o2} \frac{Y}{\left|\vec{R}_{o2}\right|} \right) + k_v \left(2Y - L_{v1} \frac{Y+b}{\left|\vec{R}_{v1}\right|} - L_{v2} \frac{Y-b}{\left|\vec{R}_{v2}\right|} \right) \\ + C_o \frac{\dot{X}Y(X+a) + \dot{Y}Y^2}{\left|\vec{R}_{o1}\right|^2} + C_v \frac{\dot{X}X(Y+b) + \dot{Y}(Y+b)^2}{\left|\vec{R}_{v1}\right|^2} = 0 \end{aligned} \tag{3.53}$$

Equations (3.52) and (3.53) clearly display nonlinearities. The relative position and velocity terms (X, Y, etc.) cannot be factored out since, for example, terms in the denominator also include X and Y as indicated in equations (3.7), (3.13), (3.18), and (3.23).

Taylor series expansion of $\vec{F}_{springs}$ and $\vec{F}_{dampers}$ is possible, as well as a duffing oscillator assumption in conjunction with an analytical solution calculation, utilizing the harmonic balance method, which is the method in (5). However, it is not the objective of this study to provide a novel approach for an analytical solution because of the high computational cost. Instead, a numerical method, Runga-Kuta to be exact, will be utilized to find solutions to the differential equations. The main focus will be the optimization in two degrees of freedom, employing genetic algorithms.

3.3. NORMALIZED STIFFNESS

Tangent stiffness is defined as the first derivative of spring force with respect to deformation. As mentioned in Section 1.2, lower values of stiffness results in better vibration isolation properties. Therefore the aim is to minimize the stiffness. Aligned with this objective, the

recovering spring force is non-dimensionalized to allow optimization operation to be independent of the size of the system.

To this effect, the following normalization is used. Position terms are normalized as

$$\hat{y} = \frac{y}{b},\ \hat{y}_b = \frac{y_b}{b},\ \hat{Y} = \hat{y} - \hat{y}_b,\ \hat{x} = \frac{x}{a},\ \hat{x}_b = \frac{x_b}{a},\ \hat{X} = \hat{x} - \hat{x}_b \tag{3.54}$$

Where all position variables are functions of time. Normalized geometric parameters are defined as

$$\alpha = \frac{b}{a},\ \beta = \frac{k_v}{k_o},\ \hat{L}_o = \frac{L_o}{a},\ \hat{L}_v = \frac{L_v}{b} \tag{3.55}$$

Equations (3.54-55) in light of Eqs. (3.7), (3.13), and (3.18-23) lead to

$$\widehat{|\vec{R}_{o1}|} = \frac{|\vec{R}_{o1}|}{a} = \sqrt{(\hat{X}+1)^2 + (\alpha\hat{Y})^2} \tag{3.56}$$

$$\widehat{|\vec{R}_{o2}|} = \frac{|\vec{R}_{o2}|}{a} = \sqrt{(\hat{X}-1)^2 + (\alpha\hat{Y})^2} \tag{3.57}$$

$$\widehat{|\vec{R}_{v1}|} = \frac{|\vec{R}_{v1}|}{b} = \sqrt{\left(\frac{\hat{X}}{\alpha}\right)^2 + (\hat{Y}+1)^2} \tag{3.58}$$

$$\widehat{|\vec{R}_{v2}|} = \frac{|\vec{R}_{v2}|}{b} = \sqrt{\left(\frac{\hat{X}}{\alpha}\right)^2 + (\hat{Y}-1)^2} \tag{3.59}$$

Recovering force in x and y directions will be taken into account separately and differentiated with respect to their corresponding axis. Defining normalized recovering forces as

$$\hat{F}_{springs_x} = \frac{F_{springs_x}}{k_o a} \tag{3.60}$$

$$\hat{F}_{springs_y} = \frac{F_{springs_y}}{k_v b} \tag{3.61}$$

Upon plugging normalized variables in Eqs. (3.54-61) into $F_{springs_x}$, Eq.), there results

$$
\begin{aligned}
F_{springs_x} = k_o \Bigg(& \left(\sqrt{a^2\left(\hat{X}+1\right)^2 + b^2\left(\hat{Y}\right)^2} - a\hat{L}_{o1} \right) \left(\frac{a(\hat{X}+1)}{a\left|\widehat{\vec{R}_{o1}}\right|} \right) \\
& + \left(\sqrt{a^2\left(\hat{X}-1\right)^2 + b^2\left(\hat{Y}\right)^2} - a\hat{L}_{o2} \right) \left(\frac{a(\hat{X}-1)}{a\left|\widehat{\vec{R}_{o2}}\right|} \right) \Bigg) \\
& + k_v \Bigg(\left(\sqrt{a^2\left(\hat{X}\right)^2 + b^2\left(\hat{Y}+1\right)^2} - b\hat{L}_{v1} \right) \left(\frac{a\hat{X}}{b\left|\widehat{\vec{R}_{v1}}\right|} \right) \\
& + \left(\sqrt{a^2\left(\hat{X}\right)^2 + b^2\left(\hat{Y}-1\right)^2} - b\hat{L}_{v2} \right) \left(\frac{a\hat{X}}{b\left|\widehat{\vec{R}_{v2}}\right|} \right) \Bigg)
\end{aligned}
\tag{3.62}
$$

Factoring a and k_o out,

$$
\begin{aligned}
F_{springs_x} = k_o a \Bigg(& \left(\sqrt{\left(\hat{X}+1\right)^2 + \alpha^2\left(\hat{Y}\right)^2} - \hat{L}_{o1} \right) \left(\frac{(\hat{X}+1)}{\left|\widehat{\vec{R}_{o1}}\right|} \right) \\
& + \left(\sqrt{\left(\hat{X}-1\right)^2 + \alpha^2\left(\hat{Y}\right)^2} - \hat{L}_{o2} \right) \left(\frac{(\hat{X}-1)}{\left|\widehat{\vec{R}_{o2}}\right|} \right) \Bigg) \\
& + k_v a \Bigg(\alpha \left(\sqrt{\left(\frac{\hat{X}}{\alpha}\right)^2 + \left(\hat{Y}+1\right)^2} - \hat{L}_{v1} \right) \left(\frac{\hat{X}}{\alpha\left|\widehat{\vec{R}_{v1}}\right|} \right) \\
& + \alpha \left(\sqrt{\left(\frac{\hat{X}}{\alpha}\right)^2 + \left(\hat{Y}-1\right)^2} - \hat{L}_{v2} \right) \left(\frac{\hat{X}}{\alpha\left|\widehat{\vec{R}_{v2}}\right|} \right) \Bigg)
\end{aligned}
\tag{3.63}
$$

Division by $k_o a$ leads to normalized recovering force in x direction

$$\hat{F}_{springs_x} = \left(\left(\sqrt{\left(\hat{X}+1\right)^2 + \alpha^2\left(\hat{Y}\right)^2} - \hat{L}_{o1} \right) \left(\frac{\left(\hat{X}+1\right)}{\left|\widehat{\vec{R}_{o1}}\right|} \right) + \left(\sqrt{\left(\hat{X}-1\right)^2 + \alpha^2\left(\hat{Y}\right)^2} - \hat{L}_{o2} \right) \left(\frac{\left(\hat{X}-1\right)}{\left|\widehat{\vec{R}_{o2}}\right|} \right) \right) + \beta \left(\alpha \left(\sqrt{\left(\frac{\hat{X}}{\alpha}\right)^2 + \left(\hat{Y}+1\right)^2} - \hat{L}_{v1} \right) \left(\frac{\hat{X}}{\alpha\left|\widehat{\vec{R}_{v1}}\right|} \right) + \alpha \left(\sqrt{\left(\frac{\hat{X}}{\alpha}\right)^2 + \left(\hat{Y}-1\right)^2} - \hat{L}_{v2} \right) \left(\frac{\hat{X}}{\alpha\left|\widehat{\vec{R}_{v2}}\right|} \right) \right) \tag{3.64}$$

Carrying out the indicated multiplications

$$\hat{F}_{springs_x} = \left(\left(\hat{X}+1\right) - \hat{L}_{o1}\frac{\left(\hat{X}+1\right)}{\left|\widehat{\vec{R}_{o1}}\right|} + \left(\hat{X}-1\right) - \hat{L}_{o2}\frac{\left(\hat{X}-1\right)}{\left|\widehat{\vec{R}_{o2}}\right|} \right) + \beta \left(\hat{X} - \hat{L}_{v1}\frac{\hat{X}}{\left|\widehat{\vec{R}_{v1}}\right|} + \hat{X} - \hat{L}_{v2}\frac{\hat{X}}{\left|\widehat{\vec{R}_{v2}}\right|} \right) \tag{3.65}$$

Equation (3.65) is simplified as

$$\hat{F}_{springs_x} = \left(2\hat{X} - \hat{L}_{o1}\frac{\left(\hat{X}+1\right)}{\left|\widehat{\vec{R}_{o1}}\right|} - \hat{L}_{o2}\frac{\left(\hat{X}-1\right)}{\left|\widehat{\vec{R}_{o2}}\right|} \right) + \beta \left(2\hat{X} - \hat{L}_{v1}\frac{\hat{X}}{\left|\widehat{\vec{R}_{v1}}\right|} - \hat{L}_{v2}\frac{\hat{X}}{\left|\widehat{\vec{R}_{v2}}\right|} \right) \tag{3.66}$$

Carrying out the same steps for $F_{springs_y}$, starting with the substitution of the normalized parameters

$$
\begin{aligned}
F_{springs_y} = k_o \Bigg(& \left(\sqrt{a^2\left(\hat{X}+1\right)^2 + b^2\left(\hat{Y}\right)^2} - a\hat{L}_{o1} \right) \left(\frac{b\hat{Y}}{a\left|\widehat{\vec{R}_{o1}}\right|} \right) \\
& + \left(\sqrt{a^2\left(\hat{X}-1\right)^2 + b^2\left(\hat{Y}\right)^2} - a\hat{L}_{o2} \right) \left(\frac{b\hat{Y}}{a\left|\widehat{\vec{R}_{o2}}\right|} \right) \Bigg) \\
& + k_v \Bigg(\left(\sqrt{a^2\left(\hat{X}\right)^2 + b^2\left(\hat{Y}+1\right)^2} - b\hat{L}_{v1} \right) \left(\frac{b(\hat{Y}+1)}{b\left|\widehat{\vec{R}_{v1}}\right|} \right) \\
& + \left(\sqrt{a^2\left(\hat{X}\right)^2 + b^2\left(\hat{Y}-1\right)^2} - b\hat{L}_{v2} \right) \left(\frac{b(\hat{Y}-1)}{b\left|\widehat{\vec{R}_{v2}}\right|} \right) \Bigg)
\end{aligned}
\tag{3.67}
$$

Factoring b and k_v out,

$$
\begin{aligned}
F_{springs_y} = k_o b \Bigg(& \frac{1}{\alpha} \left(\sqrt{\left(\hat{X}+1\right)^2 + \left(\alpha\hat{Y}\right)^2} - \hat{L}_{o1} \right) \left(\frac{\alpha\hat{Y}}{\left|\widehat{\vec{R}_{o1}}\right|} \right) \\
& + \frac{1}{\alpha} \left(\sqrt{\left(\hat{X}+1\right)^2 + \left(\alpha\hat{Y}\right)^2} - \hat{L}_{o2} \right) \left(\frac{\alpha\hat{Y}}{\left|\widehat{\vec{R}_{o2}}\right|} \right) \Bigg) \\
& + k_v b \Bigg(\left(\sqrt{\frac{1}{\alpha^2}\left(\hat{X}\right)^2 + \left(\hat{Y}+1\right)^2} - \hat{L}_{v1} \right) \left(\frac{(\hat{Y}+1)}{\left|\widehat{\vec{R}_{v1}}\right|} \right) \\
& + \left(\sqrt{\frac{1}{\alpha^2}\left(\hat{X}\right)^2 + \left(\hat{Y}-1\right)^2} - \hat{L}_{v2} \right) \left(\frac{(\hat{Y}-1)}{\left|\widehat{\vec{R}_{v2}}\right|} \right) \Bigg)
\end{aligned}
\tag{3.68}
$$

Division by $k_v b$ gives the normalized recovering force in y direction

$$\hat{F}_{springs_y} = \frac{1}{\beta}\left(\frac{1}{\alpha}\left(\sqrt{(\hat{X}+1)^2+(\alpha\hat{Y})^2}-\hat{L}_{o1}\right)\left(\frac{\alpha\hat{Y}}{\widehat{|\vec{R}_{o1}|}}\right)\right.$$
$$+\frac{1}{\alpha}\left(\sqrt{(\hat{X}+1)^2+(\alpha\hat{Y})^2}-\hat{L}_{o2}\right)\left(\frac{\alpha\hat{Y}}{\widehat{|\vec{R}_{o2}|}}\right)\Bigg)$$
$$+\left(\left(\sqrt{\frac{1}{\alpha^2}(\hat{X})^2+(\hat{Y}+1)^2}-\hat{L}_{v1}\right)\left(\frac{(\hat{Y}+1)}{\widehat{|\vec{R}_{v1}|}}\right)\right. \tag{3.69}$$
$$\left.+\left(\sqrt{\frac{1}{\alpha^2}(\hat{X})^2+(\hat{Y}-1)^2}-\hat{L}_{v2}\right)\left(\frac{(\hat{Y}-1)}{\widehat{|\vec{R}_{v2}|}}\right)\right)$$

Carrying out the indicated multiplications,

$$\hat{F}_{springs_y} = \frac{1}{\beta}\left(\hat{Y}-\hat{L}_{o1}\frac{\hat{Y}}{\widehat{|\vec{R}_{o1}|}}+\hat{Y}-\hat{L}_{o2}\frac{\hat{Y}}{\widehat{|\vec{R}_{o2}|}}\right)$$
$$+\left((\hat{Y}+1)-\hat{L}_{v1}\frac{(\hat{Y}+1)}{\widehat{|\vec{R}_{v1}|}}+(\hat{Y}-1)-\hat{L}_{v2}\frac{(\hat{Y}-1)}{\widehat{|\vec{R}_{v2}|}}\right) \tag{3.70}$$

Cancellations yield

$$\hat{F}_{springs_y} = \frac{1}{\beta}\left(2\hat{Y}-\hat{L}_{o1}\frac{\hat{Y}}{\widehat{|\vec{R}_{o1}|}}-\hat{L}_{o2}\frac{\hat{Y}}{\widehat{|\vec{R}_{o2}|}}\right)$$
$$+\left(2\hat{Y}-\hat{L}_{v1}\frac{(\hat{Y}+1)}{\widehat{|\vec{R}_{v1}|}}-\hat{L}_{v2}\frac{(\hat{Y}-1)}{\widehat{|\vec{R}_{v2}|}}\right) \tag{3.71}$$

Differentiation of (3.66) and (3.71) with respect to x and y gives directional stiffnesses. Namely,

$$\hat{K}_x = \frac{K_x}{k_o} = \frac{\partial\hat{F}_{springs_x}}{\partial\hat{X}} \tag{3.72}$$

$$\hat{K}_y = \frac{K_y}{k_v} = \frac{\partial\hat{F}_{springs_y}}{\partial\hat{Y}} \tag{3.73}$$

The above two equations yield

$$\hat{K}_x = \left(2 - \hat{L}_{o1}\frac{(\alpha\hat{Y})^2}{\widehat{|\vec{R}_{o1}|}^3} - \hat{L}_{o2}\frac{(\alpha\hat{Y})^2}{\widehat{|\vec{R}_{o2}|}^3}\right) + \beta\left(2 - \hat{L}_{v1}\frac{(\hat{Y}+1)^2}{\widehat{|\vec{R}_{v1}|}^3} - \hat{L}_{v2}\frac{(\hat{Y}-1)^2}{\widehat{|\vec{R}_{v2}|}^3}\right) \quad (3.74)$$

$$\hat{K}_y = \frac{1}{\beta}\left(2 - \hat{L}_{o1}\frac{(\hat{X}+1)^2}{\widehat{|\vec{R}_{o1}|}^3} - \hat{L}_{o2}\frac{(\hat{X}-1)^2}{\widehat{|\vec{R}_{o2}|}^3}\right) + \left(2 - \hat{L}_{v1}\frac{\hat{X}^2}{\alpha^2\widehat{|\vec{R}_{v1}|}^3} - \hat{L}_{v2}\frac{\hat{X}^2}{\alpha^2\widehat{|\vec{R}_{v2}|}^3}\right) \quad (3.75)$$

Examining equations (3.74) and (3.75), directional stiffnesses are functions of normalized relative position terms, $\hat{Y}$ and $\hat{X}$. Therefore, stiffness is not constant throughout the oscillation of the system. It can be said that each point or each $\hat{Y}$ and $\hat{X}$ pair has stiffness associated with the pair.

4. OPTIMIZATION

4.1. EXCITATION CONDITION AND OPTIMIZATION OBJECTIVE

The aim of this study is to optimize the properties of the isolation elements, so that vibration transmitted to the mass is a minimum. A general mathematical model for a point mass, supported on all four sides with springs and dampers, is given in Chapter 3. Following the mathematical model, it is necessary to define an objective for the optimization and discuss the excitation condition for which the system will be optimized. It is also helpful to point out design parameters and the range of values they can meaningfully take.

As mentioned in Section 1.2, QZS isolators are a special type of nonlinear vibration isolators with zero stiffness at equilibrium along a single axis. They were designed for disturbances acting in a single degree of freedom and were shown to be effective. However, the SDOF assumption might not be accurate in a real-life scenario. Even when the source is a lone agent, the QZS property axis and the excitation axis have to be aligned for the QZS isolator to function as designed. When these two axes are miss-aligned, it is not clear how the performance of the QZS isolator will be affected. The main argument for a performance drop is that oblique springs are designed to act as negative stiffness members, working to counteract the forces of the vertical spring, and might transmit a high level of force from the base to the mass in the horizontal direction. It is therefore considered worthwhile to focus on this aspect.

With the argument in mind, the angle between the orientation of the isolator and the axis of the excitation is depicted in Figure 4.1.

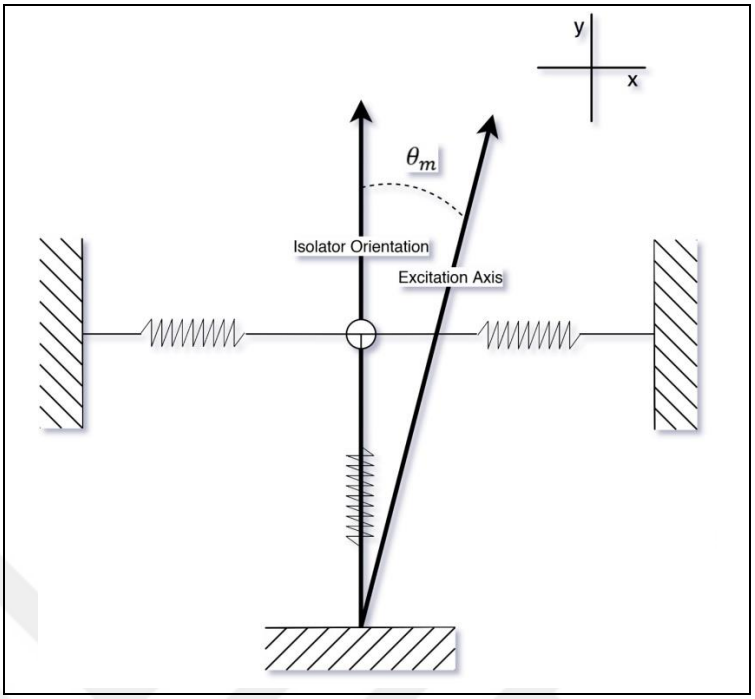

Figure 4.1. θ_m definition

x_b and y_b are components of the base excitation and, are related to the total displacement vector via the misalignment angle of θ_m as follows

$$\left|\vec{S}_{base}\right| \sin \theta_m = x_b \tag{4.1}$$

$$\left|\vec{S}_{base}\right| \cos \theta_m = y_b \tag{4.2}$$

θ_m is assumed to be smaller then 45° and the y-axis is the primary axis of excitation. These two base excitation components have a shared excitation frequency ω and have no phase difference with respect to one another.

Base excitation $\vec{S}_{base}$would cause a force $\vec{F}_T = \vec{F}_{springs} + \vec{F}_{dampers}$ to be transmitted to the mass through the transmission path of dampers and springs. The objective of the optimization is to minimize the maximum absolute transmitted force to the mass.

4.1.1. Quasi-Zero Condition

As argued before, lower values of stiffness result in better vibration isolation. To this end, a stiffness close to zero in the neighborhood of static equilibrium should provide the best result. This argument is the reason the quasi-zero-stiffness condition is favored in nonlinear vibration isolators. At static equilibrium, that is, for $x(t) \equiv 0$ and $y(t) \equiv 0$, there is no support motion and, therefore, $\hat{X}_b \equiv 0$ and $\hat{Y}_b \equiv 0$, which makes $\hat{X} = 0$ and $\hat{Y} = 0$. Substitution of these values in Eq. (3.75), where the effective stiffness in the y direction is presented, leads to

$$\widehat{|\vec{R}_{o1}|} = \widehat{|\vec{R}_{o2}|} = \widehat{|\vec{R}_{v1}|} = \widehat{|\vec{R}_{v2}|} = 1 \tag{4.3}$$

and

$$\hat{K}_y = \frac{1}{\beta}\left(2 - \hat{L}_{o1} - \hat{L}_{o2}\right) + 2 \tag{4.4}$$

To provide the QZS condition, Eq. (4.4) is set equal to zero while letting $\hat{L}_{o1} = \hat{L}_{o2} = \hat{L}_o$ for the sake of symmetry. This leads to

$$\beta + 1 = \hat{L}_o \tag{4.5}$$

Any system that satisfies equation (4.5) will have the QZS property.

Equation (4.5) indicates that for the effective stiffness in the y direction to be zero, oblique springs need to be in compression by an amount that is proportional to the ratio of the stiffnesses of oblique and vertical springs. Secondary to this point, if effective vertical stiffness is required to be softer than the sum of the two vertical springs, that is, $K_y < 2k_v$, then $\hat{K}_y < 2$ from Eq. (4.4), which would result in

$$1 \leq \hat{L}_o \tag{4.6}$$

Equation (4.6) states that oblique springs need to be in compression for the system to have a lower effective dynamic stiffness compared to a simple mass-spring system, which is the same conclusion as dictated by Eq. (4.5). This key point explains why oblique springs are

referred to as negative stiffness members and why they need to work against the vertical springs to soften the isolator and provide low dynamic stiffness.

Figure 4.2 represents some systems that satisfy Eq. (4.5) with different values of parameters α and β. The horizontal axis of the plots represents normalized vertical displacement, whereas the vertical axis represents normalized vertical effective stiffness. All six systems are for a single degree of freedom displacement, that is, $\hat{X} = 0$ for all $\hat{Y}$ values, effectively turning equation Eq. (3.75) into an SDOF equation. Playing with parameters α and β, a system can be tuned to have near-zero stiffness for a relatively wide range of $\hat{Y}$ values. However, for some applications, systems with steeper $\hat{K}_y$ curves might be desirable because steeper curves (i.e., larger stiffnesses) allow displacement response to be constrained in a narrower $\hat{Y}$ range.

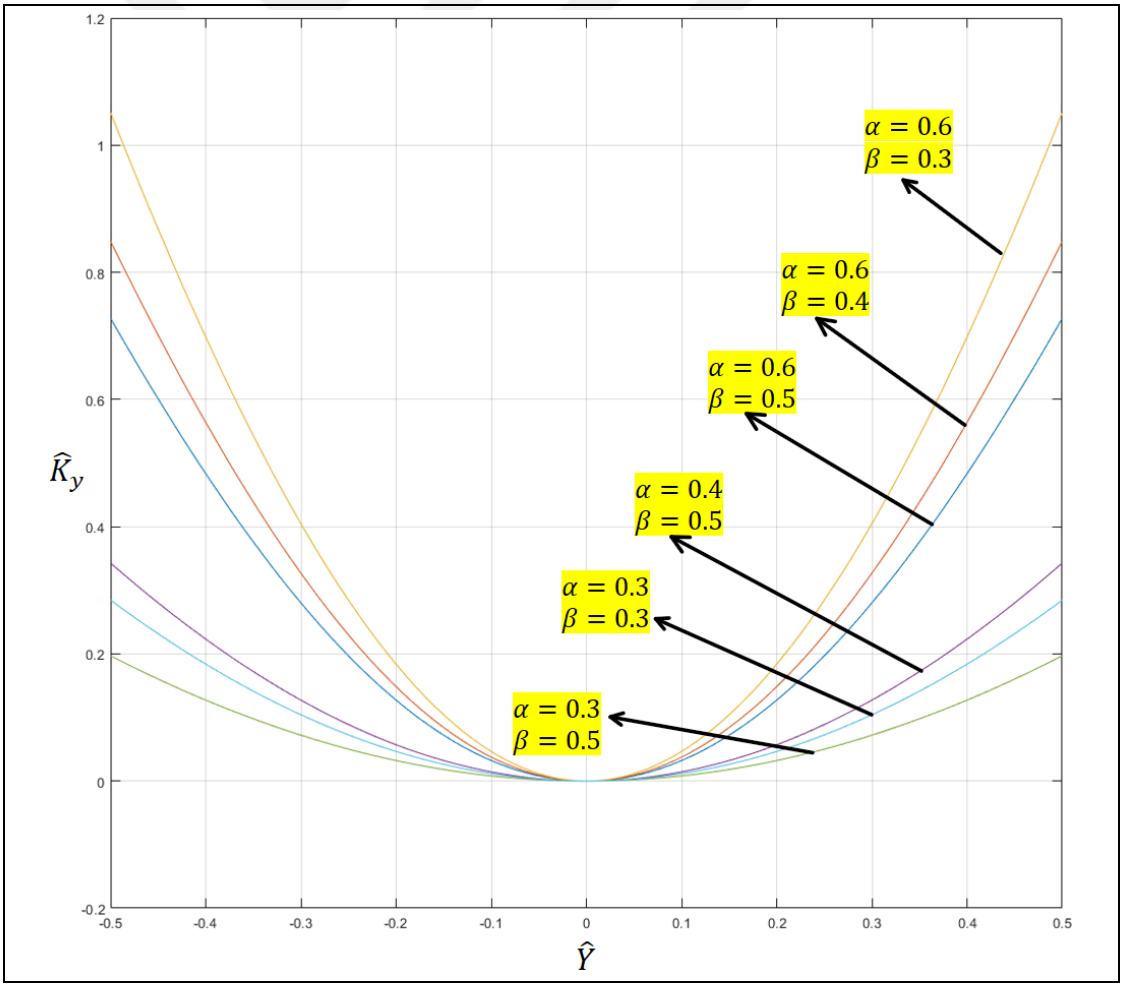

Figure 4.2 Variation of vertical stiffness in some QZS systems

If the QZS condition is to be enforced along a single axis only, the number of design parameters will be reduced. However, in light of the fact that the objective here is to optimize a nonlinear isolator with a misalignment of θ_m, it is necessary to forgo QZS along a single axis to attain a lower maximum overall transmitted displacement/force. For this reason, Eq. (4.5) need not be enforced during an optimization process. However, (4.5) may be naturally met as an outcome of the optimization process. This point is also the reason for not mentioning QZS in the thesis title but rather referring to a broader field of nonlinear isolators.

4.1.2. Static Analysis and Undeformed Spring Lengths

It is reasonable to design the system symmetrically about the x and y axes. Then, from Eq. (3.32), when the equilibrium is at point (x,y) = (0,0) because of symmetry, the effect of oblique springs cancels out and Eq. (3.32) reduces to

$$F_{springs_y} = k_v(-L_{v1} + L_{v2}) \text{ at } x = 0, y = 0 \tag{4.7}$$

Since the weight of mass m is acting downwards along the y-axis, $F_{springs_y}$ in static equilibrium needs to support the weight of mass m. This means the static deflection should equal the difference of undeformed lengths of vertical springs 1 and 2.

$$mg = k_v\Delta_{static} = k_v(L_{v1} - L_{v2}) \tag{4.8}$$

The equation

$$L_v + \Delta_{static}/2 = L_{v1} \tag{4.9}$$

holds true if $L_v = (L_{v1} + L_{v2})/2$ is defined as the average of two lengths L_{v1} and L_{v2}.

Also,

$$L_v + \Delta_{static}/2 = L_{v2} \tag{4.10}$$

Equations (4.9) and (4.10) show that L_{v1} is greater then L_v by half the amount of static deflection and L_{v2} is smaller then L_v by half the amount of static deflection while both support the weight of mass m.

Because the weight is always acting down, statically, neither mg, nor $k_v\Delta_{static}$ is represented in the equation of motion. For purposes of dynamic analysis, while symmetry about the x and y axis is preserved, we can let $L_v = L_{v1} = L_{v2}$ and $L_o = L_{o1} = L_{o2}$. However, in a real-life application, the undeformed lengths should be chosen as indicated in Eqs. (4.9) and (4.10).

4.1.3. Design Space

There are four parameters for design of a biaxial vibration isolator, namely, α, β, L_o, and L_v, definitions of which are given in (3.55). Even though the ranges of parameters are not required for mathematical optimization, they are needed for real-life applicability of the optimized parameters. However, this thesis makes no assumptions about the types of spring or spring-like components that are used. As discussed in Chapter 2, various components are used to fulfill the role of recovering force in the literature. Buckled beams, rubber mountings, and magnets are some of these examples. Even helical springs have a wide range of properties; some are only designed to work under tension, while others can both work in tension and compression. Therefore, whichever spring-like component is selected would enforce its own restrictions on the range of motion. A reasonable assumption not to include some extremes can indeed still be made. It is also true that the mathematical model doesn't cover all possible types of spring-like elements anyway. The springs of concern here have a linear relationship between their input and output.

In the study, the feasible intervals of design variables are selected somewhat arbitrarily but reasonably. As defined before, α is the geometric aspect ratio of the isolator. To prevent the isolator from being extremely slender or plump α is taken to be in the range of

$$0.1 \leq \alpha \leq 10 \tag{4.11}$$

The ratio of spring stiffnesses, β, can take a wide range of values. There is no inherent reason why two sets of springs with highly mismatched stiffnesses cannot be connected. Hence β is assumed to be in the range of

$$0.001 \leq \beta \leq 1000 \tag{4.12}$$

Normalized, undeformed length of springs $\hat{L}_v$, and $\hat{L}_o$ will govern the initial tension and compression apart from static deformation. Lengths should not take near zero values. Even a nondimensional value of 0.5 would mean springs are stretched to twice the length of their respective undeformed lengths. As argued before, this property highly depends on the type of spring used. Maximum initial tension or compression of 25% of the undeformed length is proposed.

$$0.8 \leq \hat{L}_v \leq 1.33 \text{ and } 0.8 \leq \hat{L}_o \leq 1.33 \tag{4.13}$$

4.1.4. Domain of Motion

Equations (3.74) and (3.75) that give stiffnesses in the x and y directions, respectively, are dependent on $\hat{X}$ and $\hat{Y}$. Therefore each point in the domain of $(\hat{X}, \hat{Y})$ has its own stiffness associated with it. By definition, the borders of the isolator are defined as

$$-1 \leq \hat{X} \leq 1 \text{ and } -1 \leq \hat{Y} \leq 1 \tag{4.14}$$

Because the objective of stiffness optimization is to minimize the maximum absolute transmitted displacement/force through low dynamic stiffness in both axes, and because the stiffness is dependent on displacement, optimization of $\hat{K}_x$ and $\hat{K}_y$ should be carried out simultaneously at every point inside the domain. However, optimizing for every point that satisfies Eq. (4.13) is counterproductive. A point at $\hat{X} = 1$ and $\hat{Y} = 0$ would mean a spring has collapsed entirely for all of its length, which does not make physical sense. For this reason, an initial arbitrary domain restriction is placed for optimization to be constrained inside the domain of

$$-0.5 \leq \hat{X} \leq 0.5 \text{ and } -0.5 \leq \hat{Y} \leq 0.5 \tag{4.15}$$

However, Eq. (4.15) tells nothing of the actual response domain of the mass m, that is, the region within which the mass travels during vibration. The area of the response domain may be considerably smaller. In that case, the difference between the analysis and response domains effects the simultaneous optimization process unnecessarily, which might negatively affect the isolator's performance. Due to this reason, an iterative process is implemented wherein initial optimization is carried out with Eq. (4.15). For the iterations

that follow, the response domain of the previous optimization becomes the new optimization domain for the current step until the area difference between the response domain and optimization domain is below some tolerance threshold.

4.2. STATEMENT OF THE OPTIMIZATION PROBLEM

Normalized stiffnesses for the DOFs are given in Eqs. (3.74) and (3.75) in Section 3.2. Along with these equations, design parameters and their assumed ranges are presented in Eqs. (4.11-15). As stated, a vibration isolator's objective is to minimize the transmitted force/displacement, and as also stated, designing the absorber around a low dynamic stiffness is an effective way to reach that objective. It is clear from Eqs (3.74) and (3.75) that for any given set of design parameters, the effective stiffnesses of the absorber, which are tangent stiffnesses, are not constant in the domain of motion. Instead, they are dependent on the instantaneous position of the mass center. However, for practical reasons, optimization will be carried out at discrete points, and stiffness in the neighborhood of those points will be assumed to be constant.

For isolation purposes, the time instant at which the maximum transmission of force/displacement occurs is the most crucial time instant of the response. Similarly, the most crucial point coordinate-wise is where the highest dynamic stiffness is located because a higher dynamic stiffness results in a higher transmission of force and displacement for any given set of parameters. Therefore the maximum stiffness inside the domain of motion is the benchmarking property of the governing set of parameters. The previous statement indicates that the optimization problem which is being discussed is one of minimization of the maximum.

The motion that is being analyzed is biaxial and the stiffnesses in both directions affect transmissibility. However, base motion is biased toward the y-axis via the misalignment angle θ_m. Base excitation amplitude on the two axes is presented in equations (4.1) and (4.2). It is evident that stiffnesses along the axes contribute differently to transmissibility.

An objective function with the weighted average of normalized stiffnesses is given below.

$$f = \mathrm{w_y} \times \widehat{\mathrm{K}}_\mathrm{y} + \mathrm{w_x} \times \widehat{\mathrm{K}}_\mathrm{x}\,, \text{ where } \mathrm{w_y} + \mathrm{w_x} = 1 \tag{4.16}$$

$\mathrm{w_y}$ and $\mathrm{w_x}$ are weights of normalized stiffnesses on the y and x axis, respectively, and sum up to one. Weights are calculated with the relation of

$$\mathrm{w_x} = \tan(\theta_\mathrm{m})/2 \text{ and } \mathrm{w_y} = 1 - \tan(\theta_\mathrm{m})/2\,;\ \theta_\mathrm{m} \leq \pi/4 \tag{4.17}$$

Or alternatively

$$\mathrm{w_x} = \frac{\mathrm{x_b}}{2\mathrm{y_b}} \text{ and } \mathrm{w_y} = 1 - \frac{\mathrm{x_b}}{2\mathrm{y_b}} \tag{4.18}$$

The problem is said to be the minimization of the maximum type which can be formally stated as

$$\min \ \max\{f(\widehat{\mathrm{X}}, \widehat{\mathrm{Y}}, \alpha, \beta, \hat{\mathrm{L}}_\mathrm{o}, \hat{\mathrm{L}}_\mathrm{v})\} \tag{4.19}$$

The objective function is defined at every normalized point, $\widehat{\mathrm{X}}$ and $\widehat{\mathrm{Y}}$. Coordinate pairs are discretized and numbered starting from the origin and represented with indices m and n. A discrete point is designated with P_{mn}, and the objective function for the specific discrete point P_{mn} is represented with f_{mn} given by Eq. (4.16). The optimization problem at hand is multiobjective optimization with the weighted sum method.

The set of optimized parameters for the point P_{mn} is denoted by

$$\mu_{mn} = [\alpha_{mn}\, \beta_{mn}\, \hat{L}_{o\,mn}\, \hat{L}_{v\,mn}] \tag{4.20}$$

where $m = -M, -(M-1), \dots, -1, 0, 1, \dots M-1, M$ and $n = -N, \dots, -1, 0, 1, \dots N$. In Figure 4.3, an example of a discrete domain is given, where M=N=6. For example, the point P_{24} in Figure 4.3 has stiffnesses $\widehat{\mathrm{K}}_{24_\mathrm{x}}$ and $\widehat{\mathrm{K}}_{24_\mathrm{y}}$, the objective function of f_{24} and the optimal set of parameters of μ_{24}. It is worth noting that f_{24} is not, in general, calculated using μ_{24}. f_{24} is simply the objective function being optimized at point P_{24}.

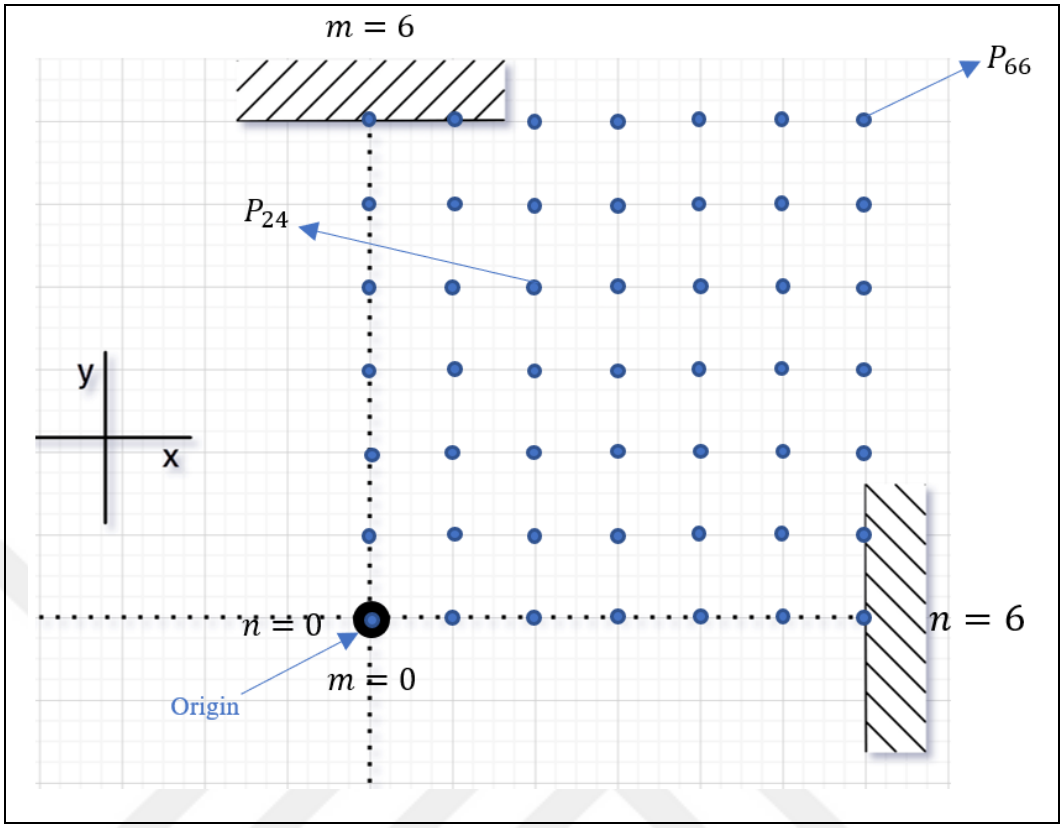

Figure 4.3. Representation of the discrete domain

The optimization process is run at each P_{mn} to calculate the optimal set of parameters μ_{mn} for that specific point by minimizing $f(\hat{X}_m, \hat{Y}_n, \alpha, \beta, \hat{L}_o, \hat{L}_v)$. The optimization needs to be performed over one quadrant of the physical domain only since the stiffness and damping elements and the geometry are symmetrical about the two axes. Every μ_{mn} is then used to calculate stiffnesses at every other point, meaning that μ_{mn}'s are being tested at every point other than the point they are being optimized for. Therefore each set of optimized parameters has its own associated set of $\hat{K}_x$'s and $\hat{K}_y$'s.

Let a matrix $\boldsymbol{\lambda_{mn}}$ of all objective functions for the first quadrant, evaluated at the values of the optimum parameter set μ_{mn}, be defined as

$$\boldsymbol{\lambda_{mn}} = \begin{bmatrix} f_{00} & \cdots & f_{0N} \\ \vdots & \ddots & \vdots \\ f_{M0} & \cdots & f_{MN} \end{bmatrix}_{\mu=\mu_{mn}} \quad ; \quad m = 0, 1, \ldots, M, \;\; n = 0, 1, \ldots, N \tag{4.21}$$

Let the maximum element of $\boldsymbol{\lambda_{mn}}$ be designated as $(\boldsymbol{\lambda_{mn}})_{max}$. The optimization process aims to minimize the maximum of all those maxima. Equation (4.19) can thus be rewritten as

$$\min \max\{(\boldsymbol{\lambda_{mn}})_{max}\}_{M,N} \tag{4.22}$$

subject to Eqs. (4.11, 12, 13, 15), which is to lead to an optimum solution over the whole domain. However, the optimum found is likely not a global optimum.

4.2.1. Nonlinear Constraints

Linear constraints on the parameters are presented in Section 4.1.3. However, to prevent negative stiffness values in the minimization process, the following additional constraints are required.

$$\widehat{\mathrm{K}}_{mn_{\mathrm{x}}}, \qquad \widehat{\mathrm{K}}_{mn_{\mathrm{y}}} \geq 0 \tag{4.23}$$

The nonlinear constraint in Eq. (4.23) prevents the system from having a softening property and possibly demonstrating a snap-thru behavior, as mentioned in Chapter 2.

4.2.2. Numeric Response Calculation and Need for Iterative Optimization

The optimization process is carried out with a built-in function of Matlab, ode45, which is based on the of Runga-Kutta method of the 4th order. The numeric solution is provided up to a suitable time duration, where the transient response dies out. The domain of motion is defined in Eq. (4.15). However, this statement is made without prior knowledge about the base motion or response with optimized parameters. The reality is that the domain in Eq. (4.15) is too large. Although the system is optimized for all points, the actual system response might exclude many of these said points, that is, in reality, the system might never pass through a significant portion of the domain. Every unnecessary point takes a toll on the optimization process described above. A set of parameters can get rejected because the maximum element of a $\boldsymbol{\lambda_{mn}}$ matrix may be located at a point where the mass never travels to.

Figure 4.4 shows the actual domain of motion or the domain of response in a hypothetical case. The area in red is where the center of mass never travels through, and optimization is unnecessary. It is clear that, before acquiring an initial set of parameters, it is not possible to solve for a response and have an idea about the shape of the response domain.

The given argument is the statement of the need for an iterative process. In which an initial domain is set according to (4.15). After the first optimization cycle, the domain of the response is calculated and fed to the next optimization cycle as the domain of motion. Iterations are continued until the optimization and real domains converge within a certain tolerance.

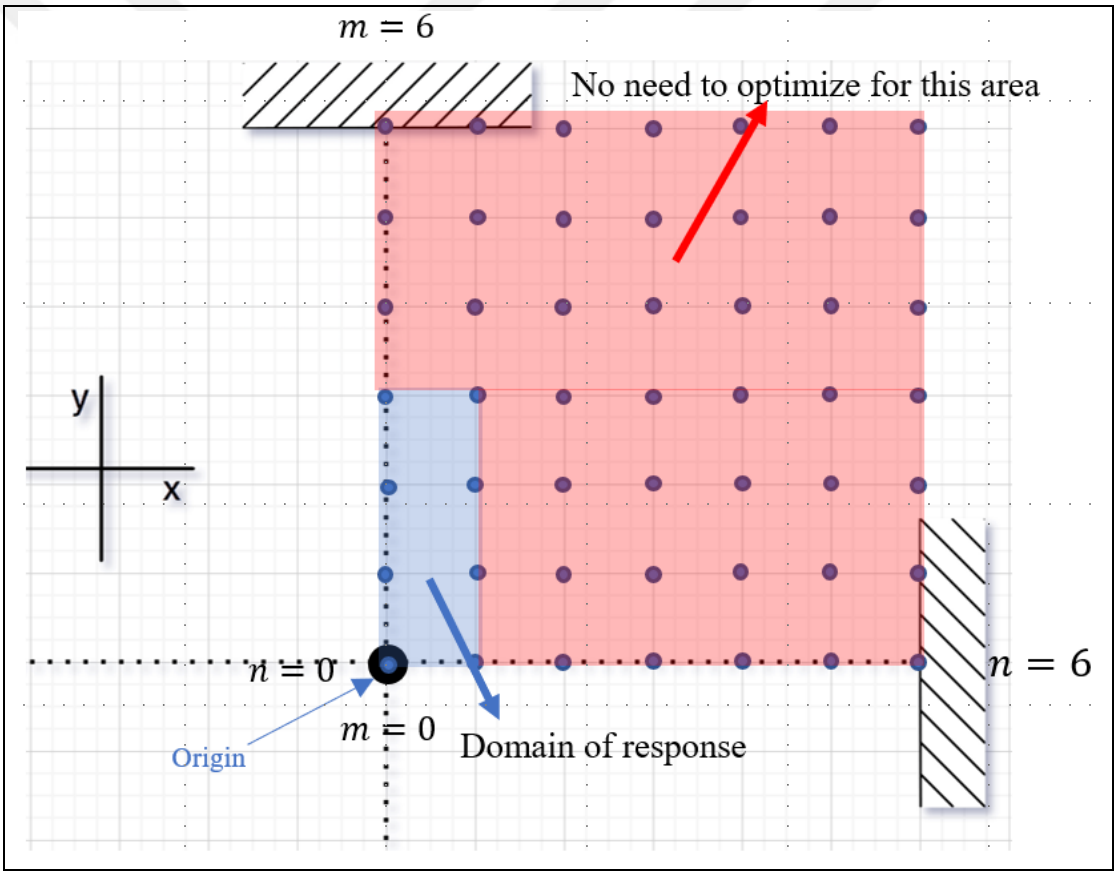

Figure 4.4. The physical domain and a hypothetical part of it wherein the motion takes place.

4.3. OPTIMIZATION ALGORITHM

A reminder and summary are considered appropriate before the optimization algorithm is laid out. Normalized stiffnesses are given in equations (3.74) and (3.75)

$$\widehat{R}_x = \left(2 - \hat{L}_{o1}\frac{(\alpha\widehat{Y})^2}{\widehat{|\vec{R}_{o1}|}^3} - \hat{L}_{o2}\frac{(\alpha\widehat{Y})^2}{\widehat{|\vec{R}_{o2}|}^3}\right) + \beta\left(2 - \hat{L}_{v1}\frac{(\widehat{Y}+1)^2}{\widehat{|\vec{R}_{v1}|}^3} - \hat{L}_{v2}\frac{(\widehat{Y}-1)^2}{\widehat{|\vec{R}_{v2}|}^3}\right) \tag{4.74}$$

$$\widehat{R}_y = \frac{1}{\beta}\left(2 - \hat{L}_{o1}\frac{(\widehat{X}+1)^2}{\widehat{|\vec{R}_{o1}|}^3} - \hat{L}_{o2}\frac{(\widehat{X}-1)^2}{\widehat{|\vec{R}_{o2}|}^3}\right) + \left(2 - \hat{L}_{v1}\frac{\widehat{X}^2}{\alpha^2\widehat{|\vec{R}_{v1}|}^3} - \hat{L}_{v2}\frac{\widehat{X}^2}{\alpha^2\widehat{|\vec{R}_{v2}|}^3}\right) \tag{4.75}$$

Where normalized denominators, $\widehat{|\vec{R}_{o1}|}$, $\widehat{|\vec{R}_{o2}|}$, $\widehat{|\vec{R}_{v1}|}$, and $\widehat{|\vec{R}_{v2}|}$ are shown to be

$$\widehat{|\vec{R}_{o1}|} = \frac{|\vec{R}_{o1}|}{a} = \sqrt{(\widehat{X}+1)^2 + (\alpha\widehat{Y})^2} \tag{4.56}$$

$$\widehat{|\vec{R}_{o2}|} = \frac{|\vec{R}_{o2}|}{a} = \sqrt{(\widehat{X}-1)^2 + (\alpha\widehat{Y})^2} \tag{4.57}$$

$$\widehat{|\vec{R}_{v1}|} = \frac{|\vec{R}_{v1}|}{b} = \sqrt{\left(\frac{\widehat{X}}{\alpha}\right)^2 + (\widehat{Y}+1)^2} \tag{4.58}$$

$$\widehat{|\vec{R}_{v2}|} = \frac{|\vec{R}_{v2}|}{b} = \sqrt{\left(\frac{\widehat{X}}{\alpha}\right)^2 + (\widehat{Y}-1)^2} \tag{4.59}$$

Functions of (3.74) and (3.75) have design parameters of

$$\alpha = \frac{b}{a},\ \beta = \frac{k_v}{k_o},\ \hat{L}_o = \frac{L_o}{a},\ \hat{L}_v = \frac{L_v}{b} \tag{4.55}$$

The weighted averages of normalized stiffnesses give birth to the objective function for a single point as

$$f = \mathrm{w_y} \times \widehat{\mathrm{K}}_{\mathrm{y}} + \mathrm{w_x} \times \widehat{\mathrm{K}}_{\mathrm{x}}\,, \text{ where } \mathrm{w_y} + \mathrm{w_x} = 1 \tag{4.16}$$

With the following linear and nonlinear constraints

$$0.8 \leq \hat{L}_v \leq 1.33,\ 0.8 \leq \hat{L}_o \leq 1.33,\ 0.1 \leq \alpha \leq 10,\ 0.001 \leq \beta \leq 1000$$
$$\widehat{\mathrm{K}}_{mn_{\mathrm{x}}},\qquad \widehat{\mathrm{K}}_{mn_{\mathrm{y}}} \geq 0 \tag{4.24}$$

Weights are calculated based on equations (4.17) and (4.18).

4.3.1. Genetic Algorithms

The method of genetic algorithms is selected for minimizing the objective function for its ease in the application of highly nonlinear problems and its robustness against local maxima or minima. However, it is a stochastic process in nature on how initial parameters are set and changed. It can be computationally costly if the genetic algorithm (GA) parameters are not appropriately adjusted for the problem in hand.

In the last decade, genetic algorithms have become a popular method due to the increase in computational power, lowering the cost of application. The technique is widely researched and documented. Hence, a detailed background won't be given here. Reference [15] go into the details of the process.

A built-in MATLAB function for a genetic algorithm, which comes with the optimization toolbox, is used. The function is designated as ga within the program. ga parameters are set based on trial and observation, considering the speed of convergence, repeatability of finding the optimal parameters, the range of spread within the population, and fitness values.

With genetic algorithms, a large population size is preferable up to a certain point, but the principle of diminishing returns applies, and larger population sizes come with an impractical computational cost for little to no gain. A population size of 200 is found to be optimal here.

The initial population is created subject to the linear constraints, and the random distribution is set to equal distribution. The fitness values of individuals are determined based on the scaling rank method. The top 10% of individuals with high fitness values are selected as

elites and directly migrated to the next generation without crossovers or mutations. The selection of individuals for the crossover step is based on roulette selection, where the probability of an individual being selected is proportional to its fitness value. The scattered crossover method is used to produce a crossover child from two individuals. Crossover children occupy the other 70% of the following generation. The last 20% is reserved for mutation children, where the mutation is set to feasible adaption, meaning mutations are restricted to be within the linear constraints. The maximum number of generations is set to 100. However, this limit is hardly ever reached. Function tolerance of 10^{-7} is the limit that usually stops the optimization process. A detailed table of GA parameters, along with the code, is provided in reference [16].

4.3.2. The Algorithm

A set of MATLAB scripts with varying functionalities are written for the optimization process. These scripts depend on each other to function. There are four main parts to all scripts. The first part is where minimization for a single point is calculated and the genetic algorithm is used. The second part is where $\boldsymbol{\lambda_{mn}}$ matrices, $(\boldsymbol{\lambda_{mn}})_{max}$ values and the best global parameters are calculated. The third part is the numeric solver, which converts normalized parameters to real values and calculates the system response. The last and fourth part is where all of the optimization processes are governed, optimization and response domains are calculated and re-adjusted until the response is within accepted tolerances. Flowchart of the set of scripts that govern the optimization process is given in Figure 4.5.

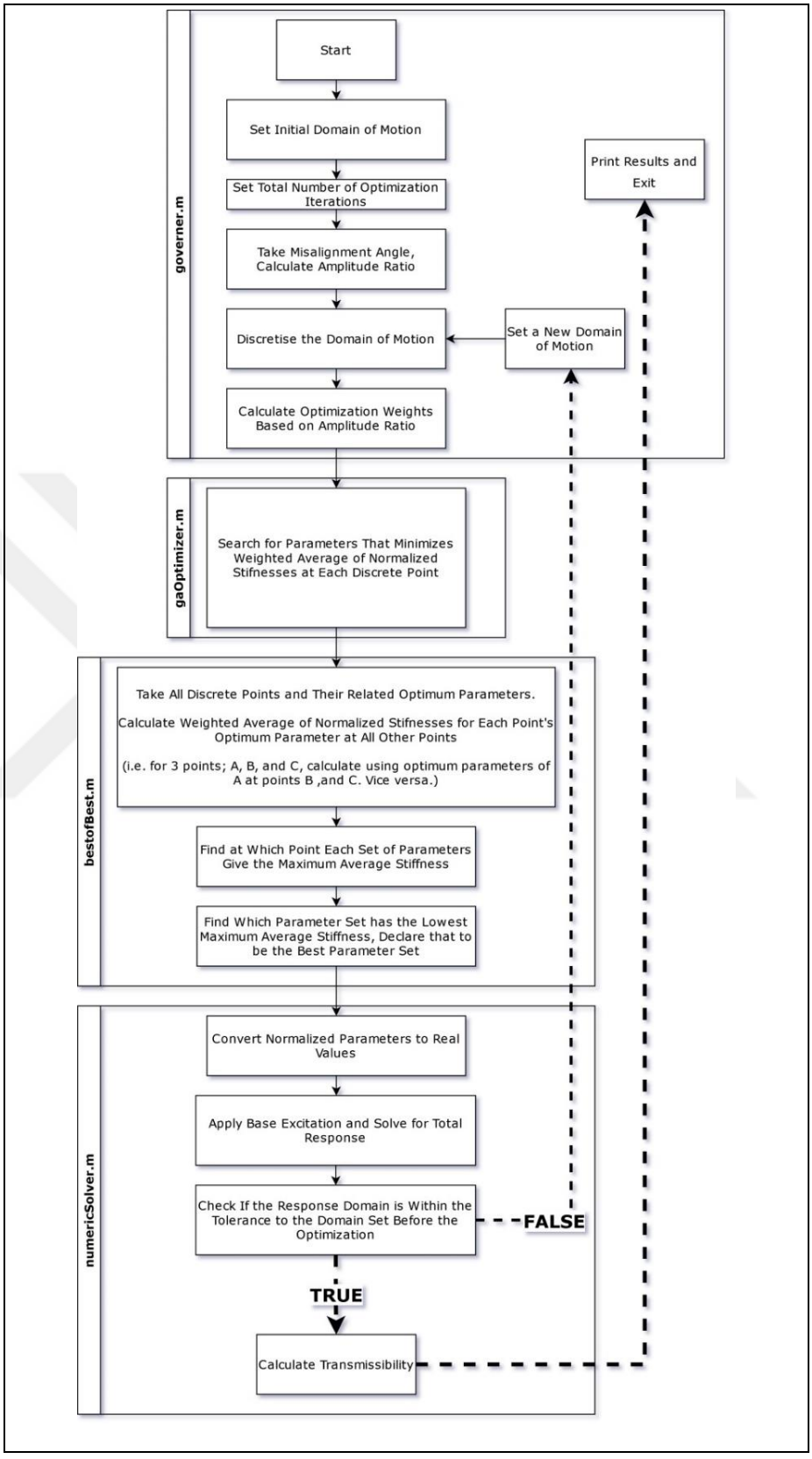

Figure 4.5 Program flowchart

The program's initialization is as follows:

- The motion domain is set to 0.5 for both axes.
- The optimization will be repeated for every point a set number of times before moving over to the next point because of the stochastic nature of genetic algorithms. A variable is set to indicate how many times the optimization should be repeated.
- The misalignment angle is taken to calculate weights for the objective function.
- The domain is discretized to a set number of divisions.
- Secondly, the program moves over to the optimization phase,
- The optimization handler is called for a point.
- Genetic algorithms run through generations until one of three conditions is satisfied. The first one is the maximum number of generations reached. The second one is the fitness of the best individual not improving beyond tolerance. The third one is the change in the parameter set being below tolerance.
- The previous step is repeated a set number of times for the same point. The best run is taken to be μ_{mn}.
- The optimization handler moves to the next point.
- Thirdly, the program calls the script called bestofBest.m, where
- $\boldsymbol{\lambda_{mn}}$ matrix, and $(\boldsymbol{\lambda_{mn}})_{max}$ for every μ_{mn} is calculated.
- Minimum of all $(\boldsymbol{\lambda_{mn}})_{max}$ is found.
- Fourthly, the minimum found above is sent to a number solver.
- Normalized parameters are converted to real values based on the mass, maximum allowed static deflection, and size limitation on the isolator.
- Response to base excitation is calculated numerically.
- The difference between the set domain of motion during the optimization process and the actual response is calculated. If the difference is larger than the tolerance, the

motion domain is re-defined, and the process starts from the beginning. Otherwise, the program terminates.

5. RESULTS

5.1. AN EXAMPLE PROBLEM

5.1.1. Problem Statement

A problem with the following conditions is considered as an example.

The isolated body has a mass of 3 kg. Base displacement is given in Eq. (5.1) and has a peak-to-peak displacement of 5 cm and a frequency of 62 rad/s. Namely,

$$S_{\text{base}} = 0.025 \sin(62t) \tag{5.1}$$

A practical restriction should be imposed for vertical springs' maximum allowed static deflection to prevent them from losing their linear elasticity. The following values are chosen arbitrarily for all isolators in the four cases that will be optimized.

$$\Delta_{static} = 0.03m, \;\; b = 0.1m \tag{5.2}$$

It is essential to investigate how different offset angles affect the optimized parameters. As mentioned before, the y-axis is the primary axis of excitation, and the maximum offset angle is limited to $\frac{\pi}{4}$. The following offset angles are considered for the optimization process.

$$\theta_m = \frac{\pi}{18}, \theta_m = \frac{\pi}{12}, \;\; \theta_m = \frac{\pi}{9}, \;\; \theta_m = \frac{\pi}{4} \tag{5.3}$$

Each offset angle has its own optimized nondimensional set of parameters. Each system is tested against the same benchmark system, which has a constant set of parameters throughout all cases.

5.1.2. Optimization of the Problem

Values of the optimization parameters are shown in Figure 5.1, which are selected with computational cost in mind. As discussed in Section 4.3.2, the parameters that govern the optimization algorithm are more numerous than those in Figure 5.1. However, these

parameters were found to be the most effective in adjusting the computation time while ensuring convergence to a minimum.

Table 5.1 Parameters of optimization

Number of Points on Each Axis	13
Total Number of Discrete Points	169
Domain Tolerance	0.001
Number of Optimization Iterations	3
Objective Function Tolerance	1e-4
Constraint Tolerance	1e-1

Parameters in Table 5.1 admittedly provide a coarse discretization; however, even with parameters in Table 5.1, the optimization process for a single case takes around 7 to 8 hours on an Intel i7 4270HQ with 12GB of RAM.

5.1.3. The Benchmark System

The benchmark system is an SDOF QZS isolator. As discussed before, the benchmark system is designed along the y-axis only. However, real world applications rarely subject a system along a single axis. Therefore, the same benchmark system will be tested in conjunction with various optimized systems, each tuned for the specified offset angle.

Benchmark system has the following nondimensional parameters, which are calculated by hand, using QZS condition in Eq. (4.5), and setting normalized stiffness $\widehat{\mathrm{K}}_{\mathrm{y}}$ to 1 at $\widehat{\mathrm{X}} = 0.5$ and $\widehat{\mathrm{Y}} = 0.5$.

$$\alpha = 0.6,\ \beta = 0.3,\ \widehat{\mathrm{L}}_{\mathrm{o}} = 1.3,\ \widehat{\mathrm{L}}_{\mathrm{v}} = 1 \tag{5.4}$$

Combining (5.4) and (5.2) reveals an isolator with real properties of

$$k_o = 2452.5\ \mathrm{N/m},\ k_v = 735.75\ \mathrm{N/m},\ \mathrm{L_o} = 21.67\ \mathrm{cm},\ \mathrm{L}_v = 10\ \mathrm{cm}$$
$$\mathrm{a} = 16.67\ \mathrm{cm}, \mathrm{b} = 10\ \mathrm{cm} \tag{5.5}$$

The equation of motion for the benchmark system, with properties given in (5.5), subjected to the excitation given in (5.1) with the offset angle $\theta_m = 0$, is solved numerically and the time history of the response is plotted in Figure 5.1.

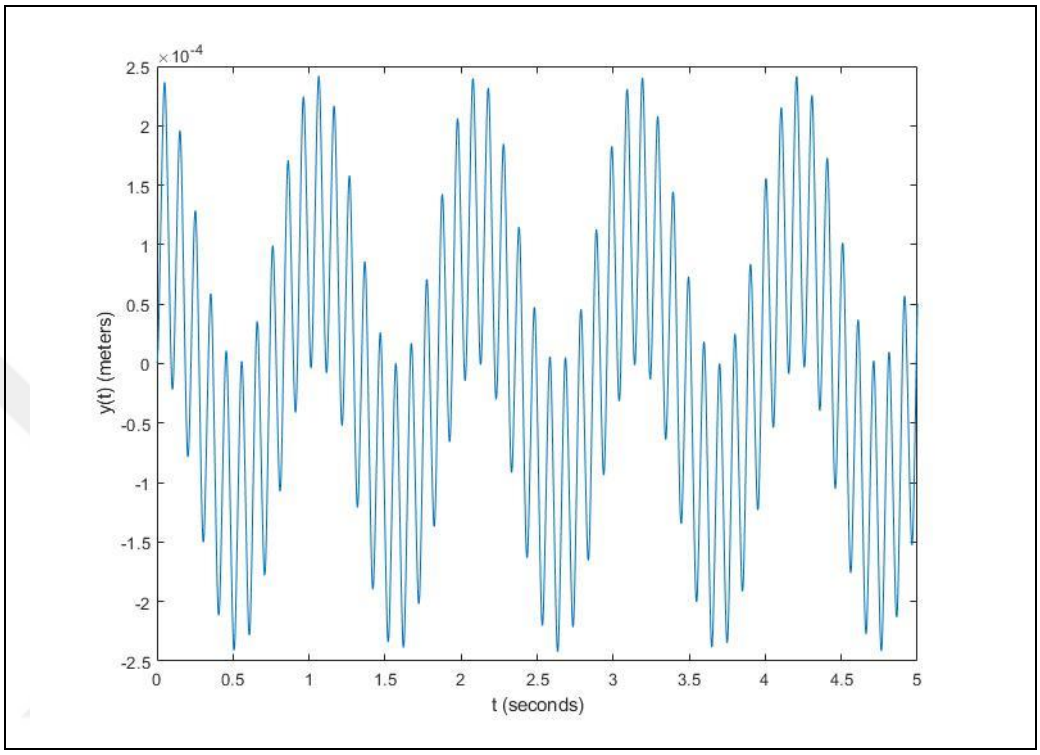

Figure 5.1. Benchmark response with zero offset

As Figure 5.1 indicates, the benchmark system's maximum amplitude of the response is calculated as 0.0242 cm. Again, this is the benchmark system's response, subjected only to an excitation along its design axis.

5.1.4. Case 1

Case 1 represents the base excitation, which is given in (5.1) with an offset angle $\theta_m = \frac{\pi}{18}$. The optimization process gives the following dimensionless parameters

$$\alpha = 1.0307,\ \beta = 0.4615,\ \hat{L}_o = 1.33,\ \hat{L}_v = 1.33 \tag{5.6}$$

Optimal physical parameter values for Case 1 follow from Eq. (5.6) as

$$k_o = 1594.4\ \text{N/m},\ k_v = 735.75\ \text{N/m},\ \text{L}_\text{o} = 12.9\ \text{cm},\ \text{L}_v = 13.3\ \text{cm}$$
$$\text{a} = 9.7\ \text{cm},\ \text{b} = 10\ \text{cm} \tag{5.7}$$

The optimum vibration response for Case 1 and the benchmark response are plotted in Figure 5.2.

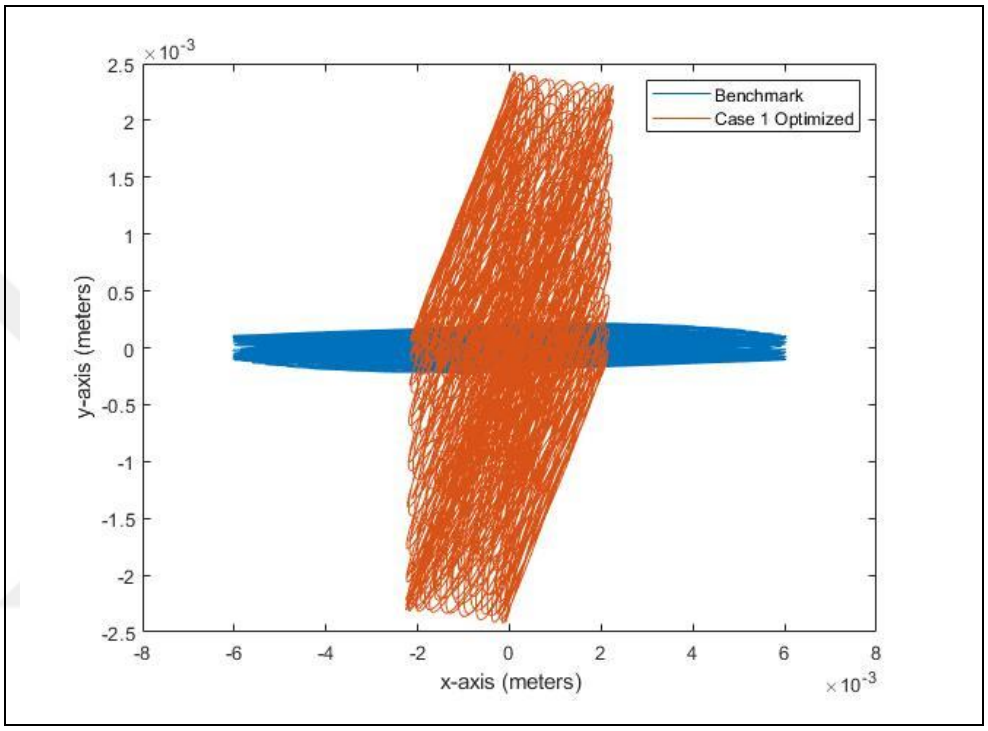

Figure 5.2. Case 1 Optimized vs. Benchmark

In the case of excitation on both axis, the maximum absolute response amplitude is calculated as

$$A = max(\sqrt{x(t)^2 + y(t)^2}) \tag{5.8}$$

The system which is optimized for Case 1, colored in orange, has a maximum absolute displacement amplitude of 0.32 cm. On the other hand, the benchmark system colored in blue, which has properties given in Eq. (5.5), has the maximum absolute response amplitude of 0.6 cm, under a base excitation with an offset angle $\theta_\text{m} = \frac{\pi}{18}$. This analysis gives an idea of how much isolation efficiency is lost due to an offset excitation on a QZS system that is designed for $\theta_\text{m} = 0$.

5.1.5. Case 2

Case 2 represents the base excitation of (5.1) with an offset angle $\theta_m = \frac{\pi}{12}$. The optimum values of the design variables are computed as

$$\alpha = 1.5455,\ \beta = 0.5889,\ \hat{L}_o = 1.33,\ \hat{L}_v = 1.33 \tag{5.9}$$

Optimal values of the physical variables for Case 2 are then calculated as

$$k_o = 1249.3\ \text{N/m},\ k_v = 735.75\ \text{N/m},\ L_o = 8.61\ \text{cm},\ L_v = 13.3\ \text{cm}$$
$$a = 6.47\ \text{cm},\ b = 10\ \text{cm} \tag{5.10}$$

The optimum vibration response for Case 2 and the benchmark response are plotted in Figure 5.3.

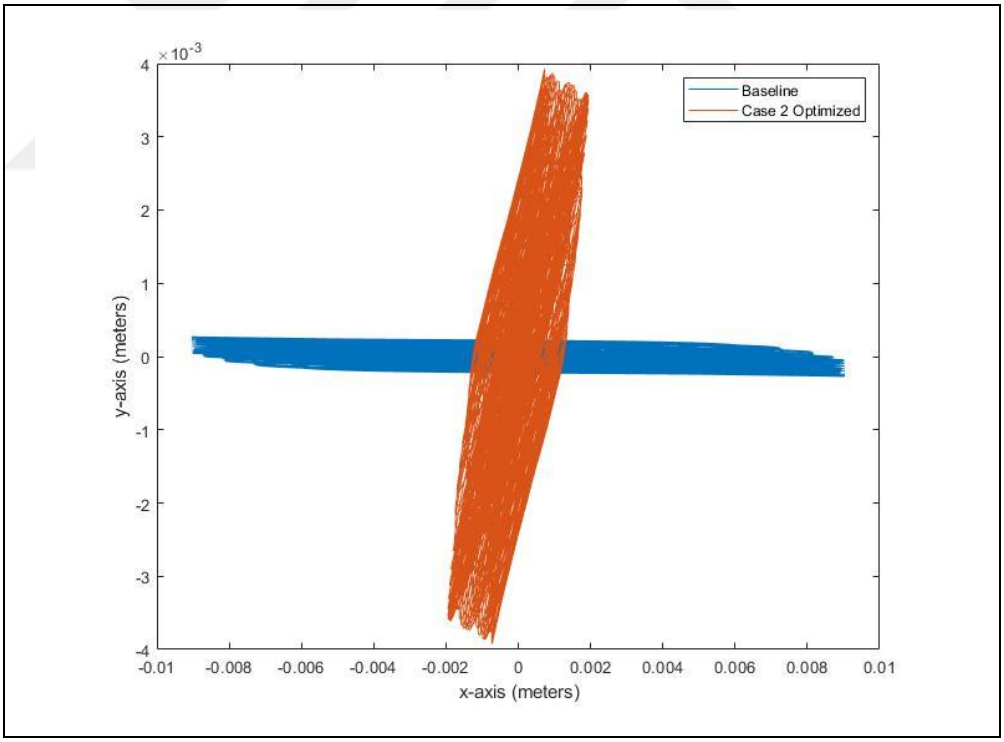

Figure 5.3. Case 2 Optimized vs. Benchmark

The system which is optimized for Case 2, colored in orange, has the maximum absolute displacement amplitude of 0.41 cm. Meanwhile, the benchmark system, colored in blue, has

the maximum absolute response amplitude of 0.9 cm, under a base excitation with an offset angle $\theta_m = \frac{\pi}{12}$.

5.1.6. Case 3

Case 3 is the base excitation in Eq. (5.1) with an offset angle of $\theta_m = \frac{\pi}{9}$. The optimum dimensionless values are computed as

$$\alpha = 2.4938,\ \beta = 0.4269,\ \hat{L}_o = 1.33,\ \hat{L}_v = 1.33 \tag{5.11}$$

Optimal physical values for Case 3 are then calculated as

$$k_o = 1723.5\ \text{N/m},\ k_v = 735.75\ \text{N/m},\ L_o = 5.33\ \text{cm},\ L_v = 13.3\ \text{cm}$$
$$a = 4.01\ \text{cm}, b = 10\ \text{cm} \tag{5.12}$$

The optimum vibration response for Case 3 and the benchmark response are plotted in Figure 5.4.

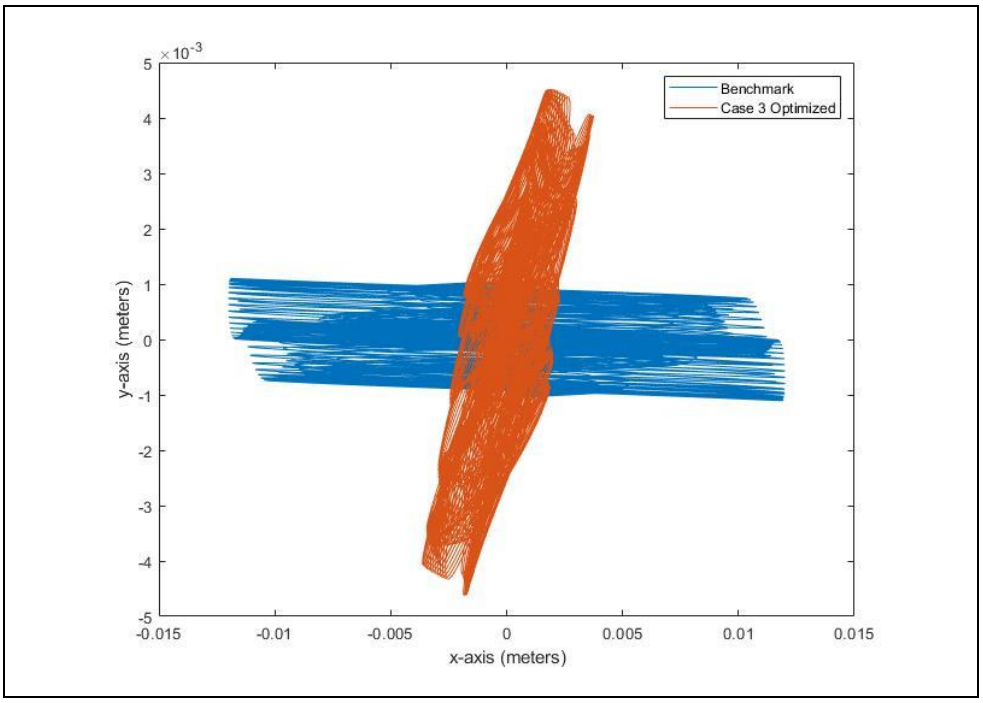

Figure 5.4. Case 3 Optimized vs. Benchmark

The system which is optimized for Case 3, colored in orange, has the maximum absolute displacement amplitude of 0.55 cm. Meanwhile, the benchmark system, colored in blue, has the maximum absolute response amplitude of 1.2 cm, under a base excitation with an offset angle $\theta_m = \frac{\pi}{9}$. As seen isolation efficiency for a QZS system drops as the offset angle is increased.

5.1.7. Case 4

Case 4 is the base excitation in Eq. (5.1) with an offset angle of $\theta_m = \frac{\pi}{4}$. The optimum values of the dimensionless design variables are computed as

$$\alpha = 1.9709,\ \beta = 0.4313,\ \hat{L}_o = 1.33,\ \hat{L}_v = 1.33 \tag{5.11}$$

Optimal physical values for Case 4 are then calculated as

$$k_o = 1706.1\ \text{N/m},\ k_v = 735.75\ \text{N/m},\ L_o = 6.75\ \text{cm},\ L_v = 13.3\ \text{cm}$$
$$a = 5.07\ \text{cm}, b = 10\ \text{cm} \tag{5.12}$$

The optimum vibration response for Case 4 and the benchmark response are plotted in Figure 5.6

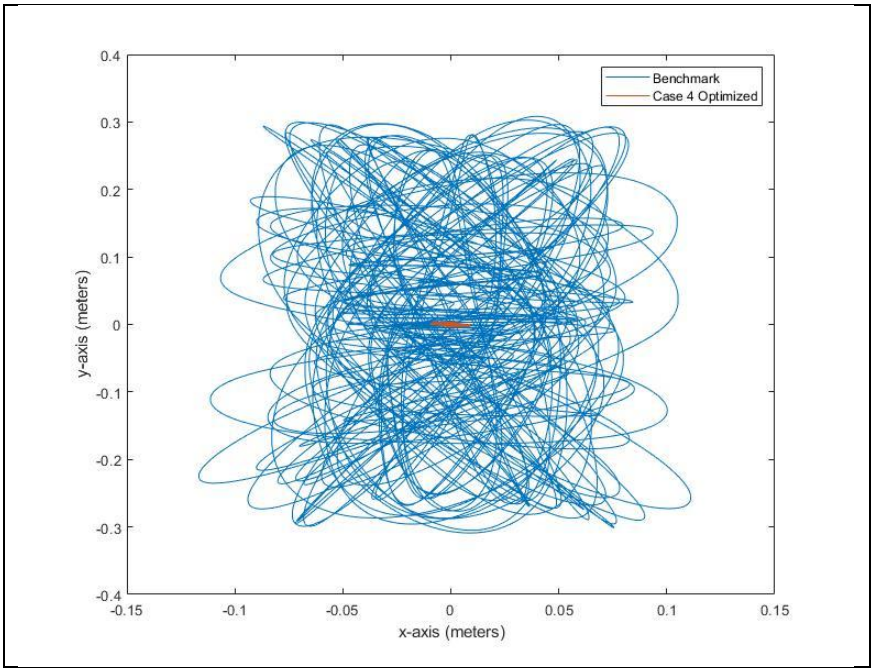

Figure 5.5. Case 4 Optimized vs. Benchmark

The system which is optimized for Case 4, colored in orange, has the maximum absolute displacement amplitude of 0.96 cm. Meanwhile, the benchmark system, colored in blue, has the maximum absolute response amplitude of 31.1 cm, under a base excitation with an offset angle $\theta_m = \frac{\pi}{4}$.

5.1.8. Summary of Results

A table that summarizes each isolator's maximum amplitude of response is given in Table 5.2.

Table 5.2 Summary of the results

Offset Angle	Benchmark	Optimized
$\theta_m = \frac{\pi}{18}$	0.6 cm	0.32 cm
$\theta_m = \frac{\pi}{12}$	0.90 cm	0.41 cm
$\theta_m = \frac{\pi}{9}$	1.2 cm	0.55 cm
$\theta_m = \frac{\pi}{4}$	31.1 cm	0.96 cm

Table 5.2 shows that the optimization approach, with the parameters in Table 5.1., leads to a reduction in isolation efficiency of approximately 70% between the offset angles of $\frac{\pi}{18}$ to $\frac{\pi}{9}$. The response of the benchmark system for $\frac{\pi}{4}$, which is 31.1 cm, goes outside the geometric boundaries of the isolator, which is not realistic.

6. CONCLUSIONS

6.1. DISCUSSION OF RESULTS

The initial expectation was that the optimized set of parameters would perform better for all offset angles, with the performance margin increasing as the angle increased. Although the optimized systems performed better under all cases; the performance margins did not increase with offset angle. Parameters derived from the proposed method resulted in a steady reduction in isolation efficiency for angles $\frac{\pi}{18}$, $\frac{\pi}{12}$ and $\frac{\pi}{9}$. This might indicate that the real sets of optimized parameters haven't been found for some or all investigated cases.

The benchmark system performs significantly worse along the x-axis, as expected. The reason is that QZS systems have precompressed oblique springs, significantly stiffer than their vertical counterparts, to work as negative stiffness members. These oblique springs are not designed with force transmission along the x-axis in mind. Therefore, misalignment between the design and excitation axis causes high levels of mass displacement along the x-axis.

For small angles, although not precisely equal, the real optimal set of parameters should be close to the benchmark because a QZS system is expected to be the best-performing system on single-axis excitation. Therefore it is reasonable to expect a set of parameters that approximate a QZS system for small angles, and the optimal system, should diverge from QZS as the angle grows. With this argument in mind, if the optimized set of parameters for Case 1, given in (5.6), is considered, it can be seen that the condition of QZS given in (4.5), $0.4615 + 1 = 1.4615 \approx 1.33$ is nearly satisfied.

Case 4 had the offset angle of $\theta_m = \frac{\pi}{4}$. The benchmark system had an unbounded response, exceeding the geometric restrictions of the isolator.

There is a clear tradeoff between allowing displacement transmission along one of the axis compared to the other one. Optimized systems, in all but the last case, performed better along the x-axis, to the detriment of the performance along the y-axis, compared to the benchmark. This might also indicate that there are more than one optimal set of parameters that calculates the same $max(\sqrt{x(t)^2 + y(t)^2})$, trading off between x-axis response and y-axis response.

6.2. POSSIBLE SHORTCOMINGS OF THE ALGORITHM

There are three main shortcomings of the proposed algorithm. These are,

The real optimal parameter set is possibly not associated with any discrete point.

The weight assignment method might not be optimal.

How the domain tolerance is defined might cause a handicap.

Firstly, as explained in Chapter 4, each optimized set is associated with a discrete point. The resulting weighted stiffness value of the set is then calculated at all other points, and the maximum weighted stiffness value is flagged as the defining value of that set. Whichever set has the minimum weighted stiffness value is declared to be the most optimal set for the given problem. However, it is possible that the most optimal real set has no association with any discrete points. That is not to say that the real optimized set would reveal itself if the number of discrete points is increased. The argument here has nothing to do with the numerical limitations of the problem. The real optimized set might be a set that does not produce the minimum weighted stiffness at any single point but when calculated at all points, has the minimum of maximum weighted stiffness. If that is the case, then the proposed algorithm cannot be expected to find the real optimal set.

Secondly, weights associated with the weighted stiffnesses, and hence the objective function, are calculated based on the base excitation amplitude ratios. Therefore, the relation between the amplitude ratios and the weights is a linear one. Thus, how much the minimization of the stiffness along one axis is favored against the other one is also in a linear relationship to the excitation amplitude ratio. However, whether this relationship should be linear or not isn't clear.

Thirdly, the main objective of defining an optimization domain tolerance was to be free of unnecessary nonlinear constraints by not including points that are not located within the system's response. This discussion point is connected to the first one. By changing the domain of motion and re-running the optimization process, not only the unnecessary constraints are excluded, but sometimes a better parameter set may also be missed. This, in turn, causes the system's response to be magnified and the domain of motion to grow rather than shrink on the next iteration. There have been some examples observed which

demonstrate this behavior. If the domain of motion oscillates between growing and shrinking cysles with each iteration, the optimization process cannot converge to a solution.

6.3. SUGGESTIONS

For a 2DOF problem, it might be beneficial to use the suggested method, depending on the displacement transmission tolerances for a given problem. The method can prove to be even more beneficial if the optimization algorithm parameters given in Table 5.1 are fine-tuned and the number of discrete points is increased.

When it comes to improving the method, bypassing all the stiffness calculations and the normalized parameters by directly feeding design parameters into the genetic algorithm, with a numeric solver as the objective function feedthrough, would solve all the shortcomings of the current method, discussed in Section 6.2. However, the computational cost would be some order of magnitude higher than the proposed method.

7. REFERENCES

1. Carrella A, Brennan MJ, Kovacic I, Waters TP. On the force transmissibility of a vibration isolator with quasi-zero-stiffness. J Sound Vib. 2009;322(4–5):707–17.

2. Daniel J. Inman. Engineering Vibration. Fourth Edition. Pearson; 2014.

3. Ibrahim RA. Recent advances in nonlinear passive vibration isolators. J Sound Vib. 2008;314(3–5):371–452.

4. Carrella A. Passive vibration isolators with high-static-low-dynamic-stiffness. 2008;226. Available from: http://eprints.soton.ac.uk/id/eprint/51276

5. Carrella A, Brennan MJ, Waters TP, Lopes V. Force and displacement transmissibility of a nonlinear isolator with high-static-low-dynamic-stiffness. Int J Mech Sci [Internet]. 2012;55(1):22–9. Available from: http://dx.doi.org/10.1016/j.ijmecsci.2011.11.012

6. Kovacic I, Brennan MJ, Waters TP. A study of a nonlinear vibration isolator with a quasi-zero stiffness characteristic. J Sound Vib. 2008 Aug 19;315(3):700–11.

7. Zheng Y, Zhang X, Luo Y, Yan B, Ma C. Design and experiment of a high-static-low-dynamic stiffness isolator using a negative stiffness magnetic spring. J Sound Vib [Internet]. 2016;360:31–52. Available from: http://dx.doi.org/10.1016/j.jsv.2015.09.019

8. Huang X, Liu X, Sun J, Zhang Z, Hua H. Vibration isolation characteristics of a nonlinear isolator using euler buckled beam as negative stiffness corrector: A theoretical and experimental study. J Sound Vib [Internet]. 2014;333(4):1132–48. Available from: http://dx.doi.org/10.1016/j.jsv.2013.10.026

9. Abolfathi A. Nonlinear vibration isolators with asymmetric stiffness. 2012;237.

10. Sun X, Jing X. Multi-direction vibration isolation with quasi-zero stiffness by employing geometrical nonlinearity. Mech Syst Signal Process [Internet]. 2015;62:149–63. Available from: http://dx.doi.org/10.1016/j.ymssp.2015.01.026

11. Alabuzhev PM. Vibration protection and measuring systems with quasi-zero stiffness. CRC Press; 1989.

12. Carrella A, Brennan MJ, Waters TP. Static analysis of a passive vibration isolator with quasi-zero-stiffness characteristic. J Sound Vib. 2007;301(3–5):678–89.

13. Ravindra B, Mallik K. Performance of Non-Linear Vibration Isolators Under Harmonic Excitation. J Sound Vib. 1994;170(3):325–37.

14. Worden K. On Jump Frequencies in the Response of the Duffing Oscillator. Vol. 198, Journal of Sound and Vibration. 1996.

15. MathWorks. How the Genetic Algorithm Works [Internet]. [cited 2022 Oct 30]. Available from: https://www.mathworks.com/help/gads/how-the-genetic-algorithm-works.html

16. Sarp Gönülkırmaz. Codebase [Internet]. Github. 2022 [cited 2022 Oct 30]. Available from: https://github.com/AeonLightyear/2DOFNonLinearIsolatorOpt